PP PHYSICS AT LHC

L. BRAVINA (UIO),

IN COLLABORATION WITH

A.B.KAIDALOV, K. BORESKOV, O.V. KANCHELI, K.TYWONIUK, I. ARSENE,

J. BLEIBEL, G. EYYUBOVA, R.KOLEVATOV,

L. MALININA, M.S. NILSSON, E. ZABRODIN

1sr International Conference on New Frontiers in Physics 2012, OAC, Kolymbari, Crete

1. Gluon shadowing

OSLO THEORY GROUP

6. Equation of State

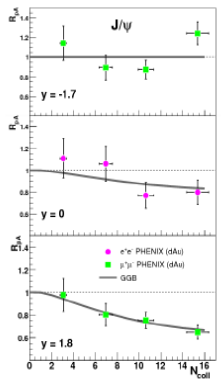

- shadowing in agreement with data at RHIC
- first signal of coherent HQ production?
- at LHC - strong IS effect!

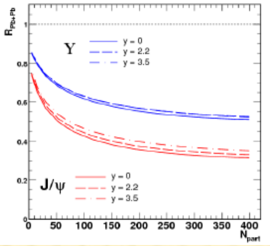

4. Freeze-out

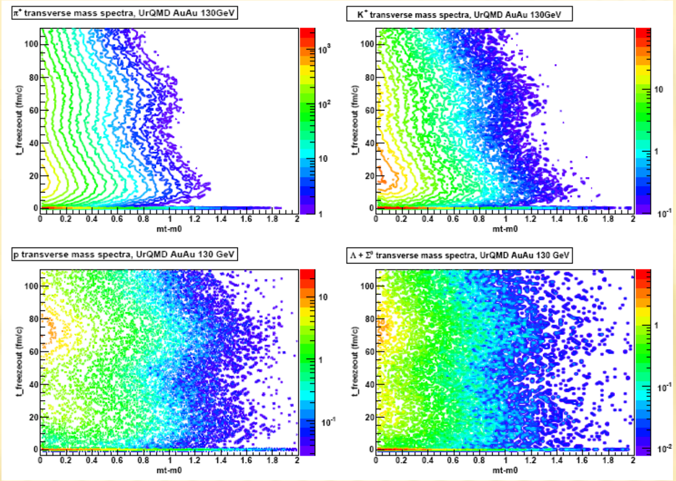

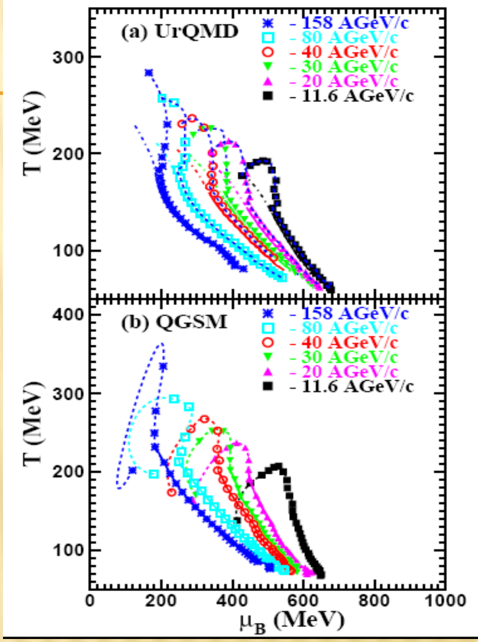

2. Elliptic flow

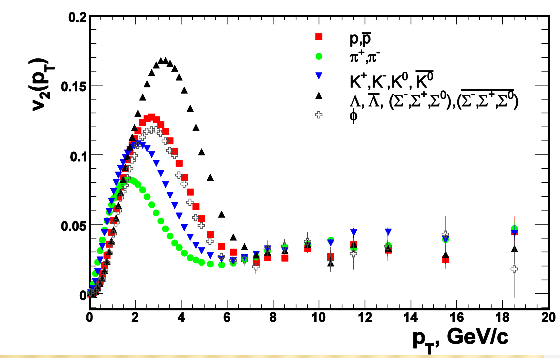

5. HBT correlations

7. Predictions for pp

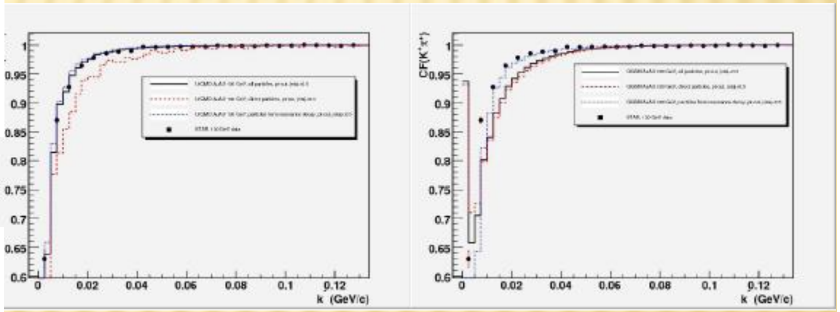

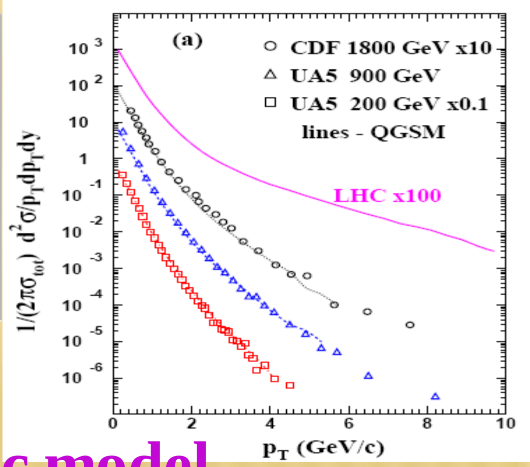

3. HYDJET++

- realistic nuclear geometry
- describes well RHIC data on high-p_T
- well suited for LHC energies
- basic MC tool for CMS HI analysis, also used by ALICE

8. Flow in pp 9. Regge field theory and stochastic model

10. Di-hadron azimuthal correlations and ridge.

CONTENT:

1. Motivations

2. Quark Gluon String Model for pp collisions at LHC: spectra, multiplicity distributions, forward-backward correlations

3. Freeze-out and Femptoscopic correlations in pp collisions: influence of resonances, minijets and formation time

4. Flow in pp and AA : as initial state effect

Conclusions

Observation of Long-Range, Near-Side Angular Correlations in Proton-Proton Collisions at the LHC

JHEP 1009:091,2010
Sep 2010. e-Print: **arXiv:1009.4122** [hep-ex]
CMS Collaboration,

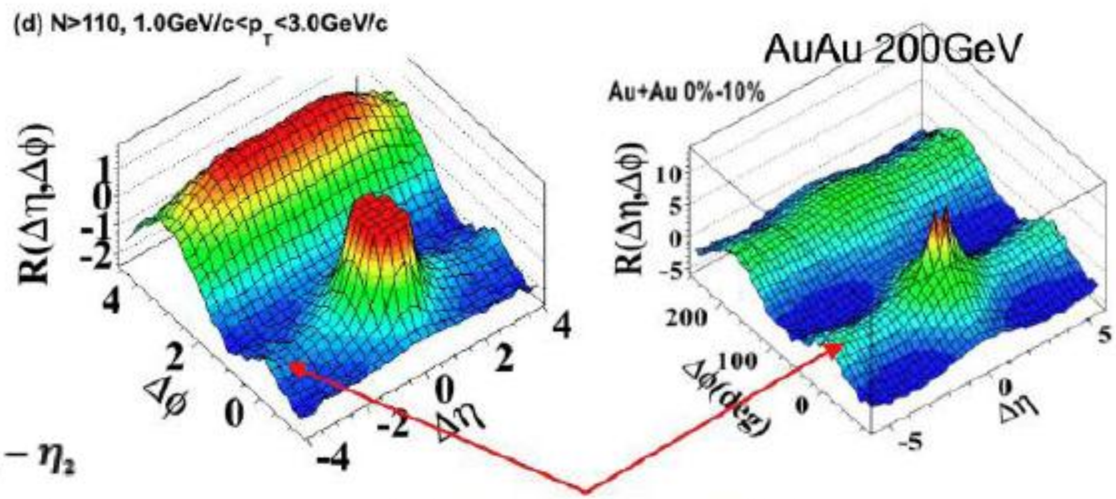

okhtin,

$\Delta\eta = \eta_1 - \eta_2$

$\Delta\varphi = \varphi_1 - \varphi_2$

Similar "ridge" in high multiplicity pp
(even similar p_T dependence)

Signal is observed at large difference $|\Delta\eta| < 4.8$, large multiplicity N > 90 and at medium particle transverse momentum 1 < pT < 3 GeV/c.

2. QGSM PREDICTIONS FOR PP AT LHC

A.B. Kaidalov, K.A.Ter-Martirosyan, PLB 117 (1982)
N.S.Amelin, L.B., Sov.J.Nucl.Phys. 51 (1990) 133
N.S.Amelin, E.F.Staubo, L.P.Csernai, PRD 46 (1992) 4873

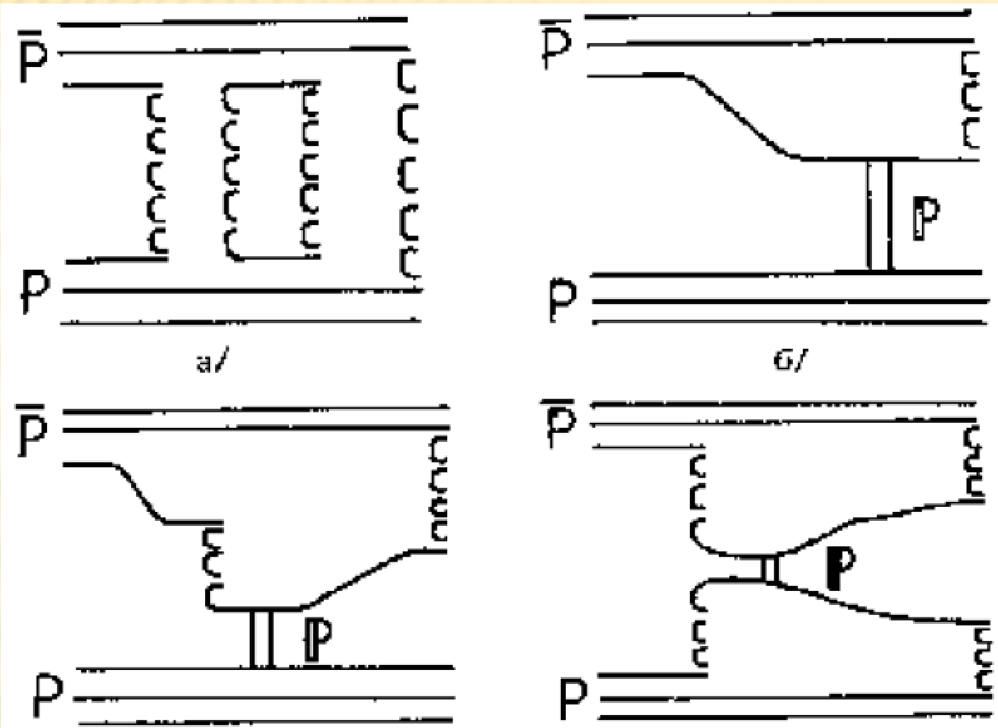

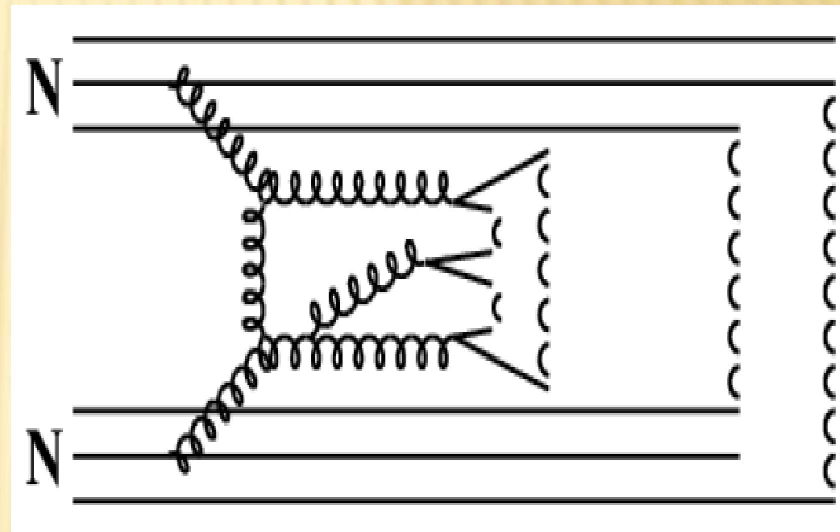

At ultra-relativistic energies: multi-Pomeron scattering, single and double diffraction, and jets (hard Pomeron exchange)

Gribov's Reggeon Calculus + string phenomenology

Regge poles in QCD.

Large distance phenomenon. Nonperturbative methods should be used.

- 1/N – expansion in QCD. H.t`Hooft, G.Veneziano

Expansion of amplitudes in terms of the small parameter 1/N, where $N=N_c \approx N_f$.

Diagrams are classified according to their topology.

The first term – planar diagrams.

Planar diagrams.

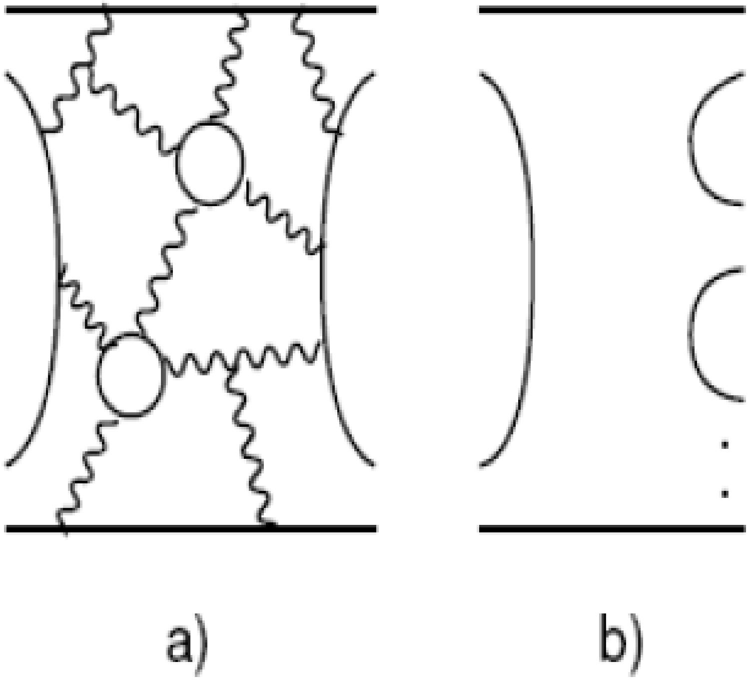

Exchange by valence quarks in the t-channel.

At large energies they correspond to ρ,ω,f,.. exchanges.

Contributions to total cross sections decrease as $s^{(\alpha_R(0)-1)} \approx 1/\sqrt{s}$

Pomeron in 1/N-expansion.

In 1/N-expansion the Pomeron corresponds to the cylinder-type diagrams.

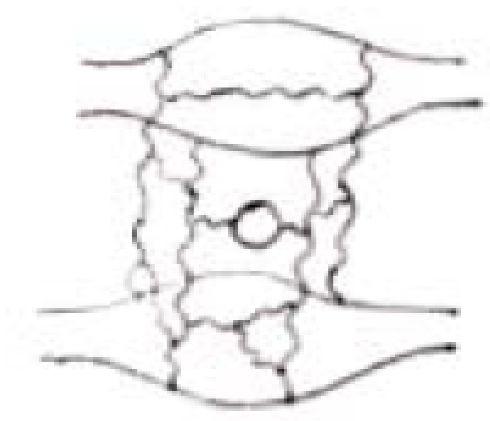

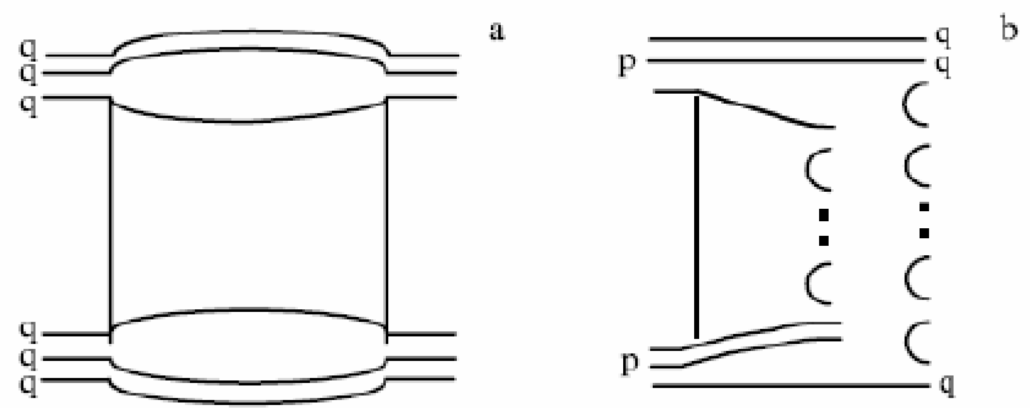

$$T_{pl} \sim 1/N \qquad T_{cyl} \sim 1/N^2$$

$$T_{n_b,n_h} \sim \left(\frac{1}{N}\right)^{n_b+2n_h}$$

n_b - number of boundaries,

n_h – number of holes

Multiparticle production and topological expansion.

Cuttings of many pomerons in 1/N- expansion correspond to multi-chain configurations

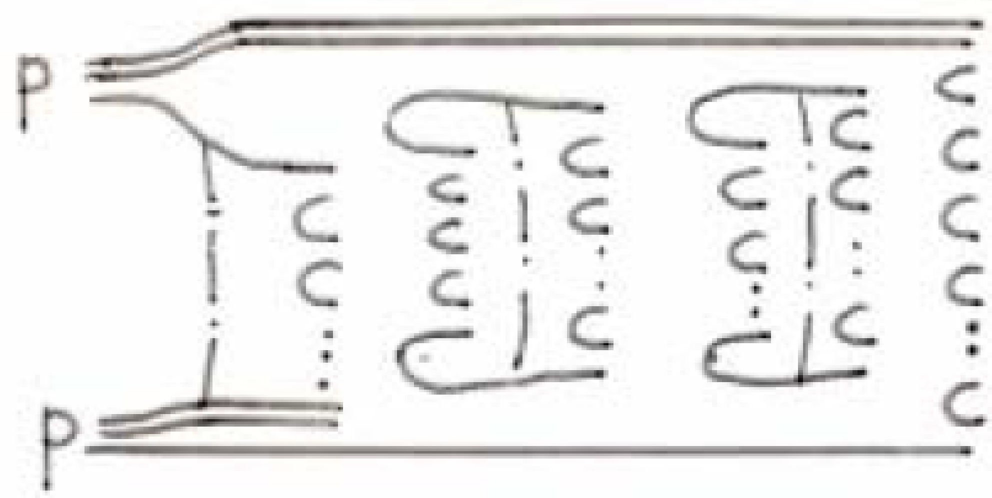

Extra chains due to sea-quarks or gluons in colliding hadrons

Quark-Gluon Strings Model.

Models of multi-particle production, based on reggeon calculus, 1/N-expansion and string dynamics:

Dual Parton Model (DPM) – Orsay,

Quark-Gluon Strings Model (QGSM) – ITEP

AGK-cutting rules determine the weights of 2k-chains configurations.

Rapidity and multiplicity distributions of final hadrons in chains can be determined theoretically.

Inclusive spectra

$$\frac{d\sigma^h}{dy} = \sum_{k=0}^{\infty} \sigma_k(\xi)\, \varphi_k^h(\xi, y) \quad ; \qquad \xi \equiv \ln\frac{s}{s_0}$$

σ_k cross section for 2k chains production

Multiplicity distribution (k=0 - diffraction)

$$\sigma_n(\xi) = \sum_{k=0}^{\infty} \sigma_k(\xi)\, W_n^k(\bar{n}_k(\xi))$$

Consider as an example $pp \to hX$

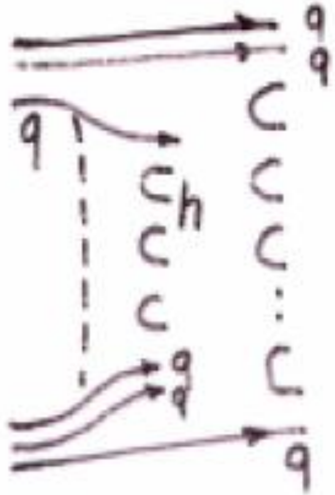

In the fragmentation region

$$\frac{x}{\sigma_2}\frac{d\sigma_2^h}{dx} = \int_x^1 dx_1\, f_p^{q(2)}(x_1)\, D_q^h\left(\frac{x}{x_1}\right)\frac{x}{x_1} +$$

+ contrib. from second chain

$x = 2p_{\parallel}/\sqrt{s} \equiv x_F$

$f_p^{q(2)}(x_1)$ determines how energy is devided between q and qq - chains

$$f_p^{qq(2)}(x_1) = f_p^{q(2)}(1 - x_1)$$

Inclusive spectra of different hadrons are determined by the fragmentation functions $D_i^h(z)$. From planar diagrams:

$$z D_u^{\pi^+}(z) = \begin{cases} a^{\pi} & , \quad z \to 0 \\ C^{\pi^+}(1-z)^{-\alpha_R + \lambda} & , \quad z \to 1 \end{cases}$$

$$z D_u^{\pi^-}(z) = \begin{cases} a^{\pi} & , \quad z \to 0 \\ C^{\pi^-}(1-z)^{-\alpha_R + \lambda + 1} & , \quad z \to 1 \end{cases}$$

$2(1-\alpha_R(0))$

$\lambda = 2\alpha_R' \cdot \overline{p_{\perp\pi}^2} \approx 0.5 \quad , \quad \alpha_R \equiv \alpha_R(0) = 0.5$

$(\tilde{D}_i^h(z) \equiv D_i^h(z)/a^h)$

Interpolation formulas for $D_i^h(z)$

e.g.

$$z D_u^{\pi^+}(z) = a^{\pi}(1-z)^{-\alpha_R+\lambda}$$

$$z D_u^{\pi^-}(z) = a^{\pi}(1-z)^{-\alpha_R+\lambda+1}$$

$$z D_u^{K^+}(z) = a^{K}(1-z)^{-\alpha_\varphi(0)+\lambda_K} \cdot (1+b_K z) \; ; \quad \alpha_\varphi(0) \simeq 0$$

$$z D_u^{\bar{D}^0}(z) = a^{D}(1-z)^{-\alpha_\psi(0)+\lambda_D} \cdot (1+b_D z)$$

Constants a^{π}, a^{K}, b_K can be determined theoretically.

$$a^{\pi} = 0.44$$

$$a^{K}/a^{\pi} \simeq 0.12$$

Constraints due to energy-momentum, S, B, Q,.. conservation allow one to fix parameters in many cases.

No free parameters!

The model has correct double ($x \rightarrow 0$) and triple ($x \rightarrow 1$) Regge limits.

Multiplicity distribution for a single cut Pomeron is of Poisson-type. Summary distribution is much broader.

QGSM PREDICTIONS and RESULTS FOR LHC

Inelastic collisions **NSD collisions**

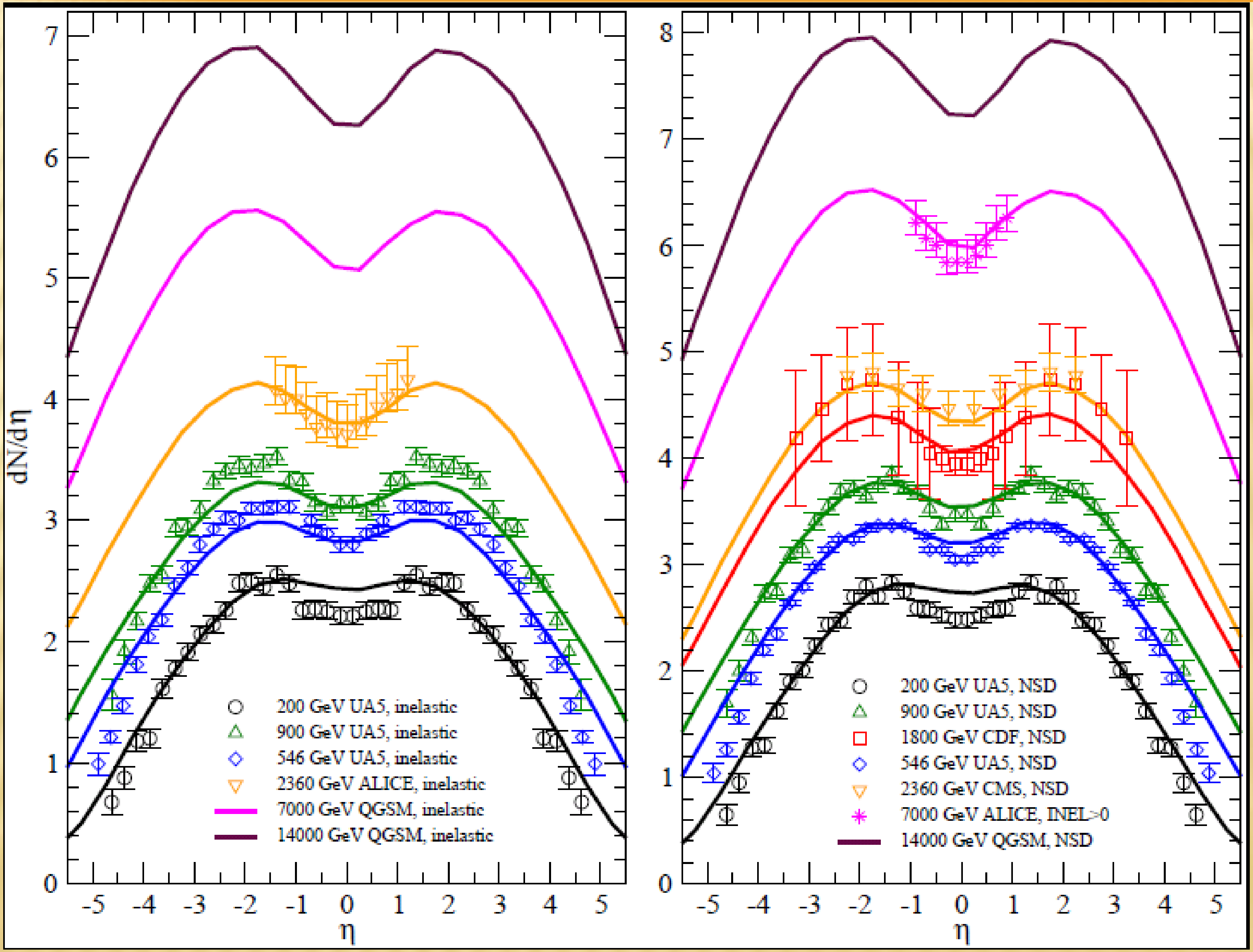

J.Bleibel. L.B. et al., (work in progress)

QGSM PREDICTIONS and RESULTS FOR LHC

Transverse momentum distributions

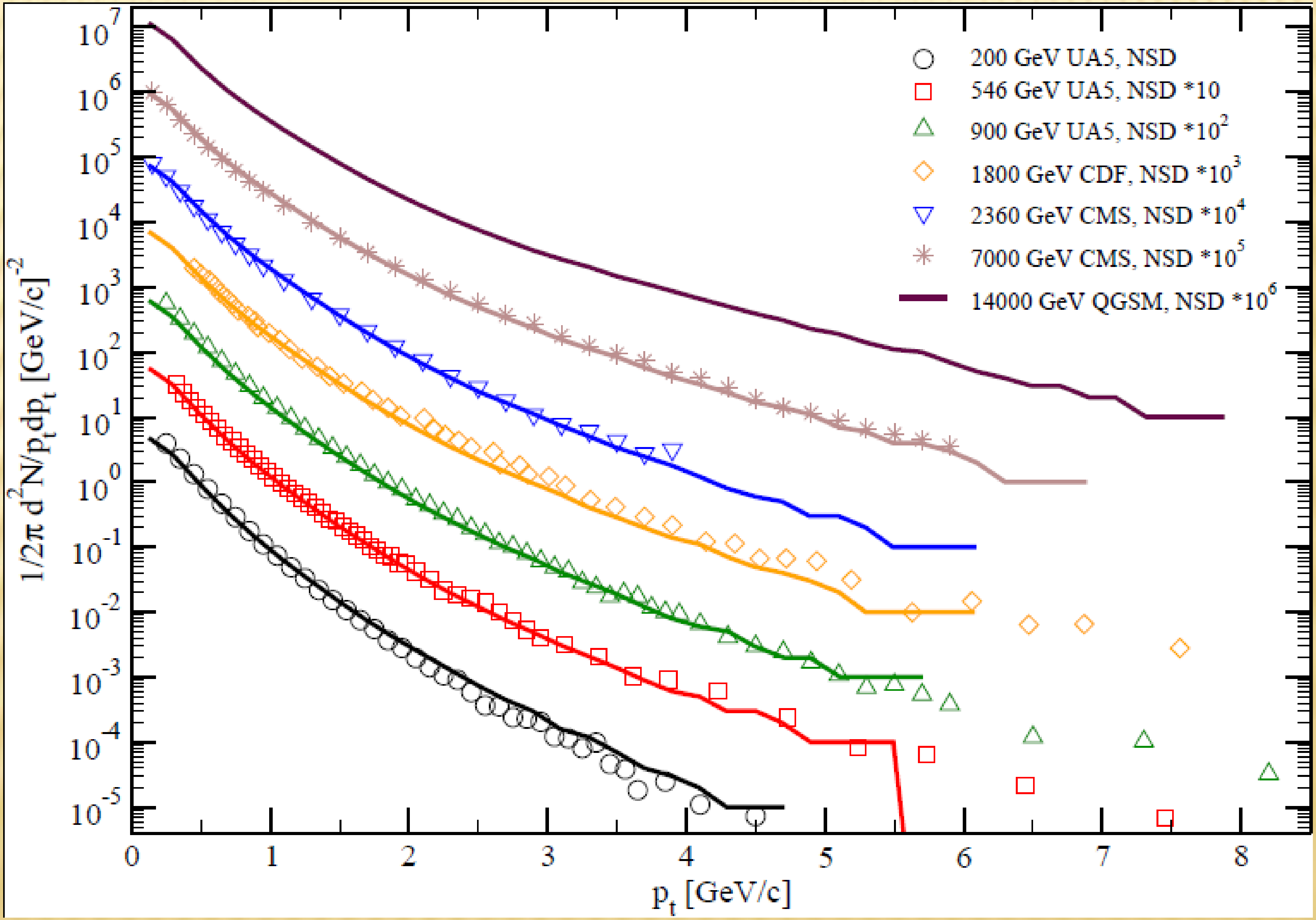

J.Bleibel, L.B. et al. (work in progress)

QGSM PREDICTIONS and RESULTS FOR LHC

Transverse momentum distributions

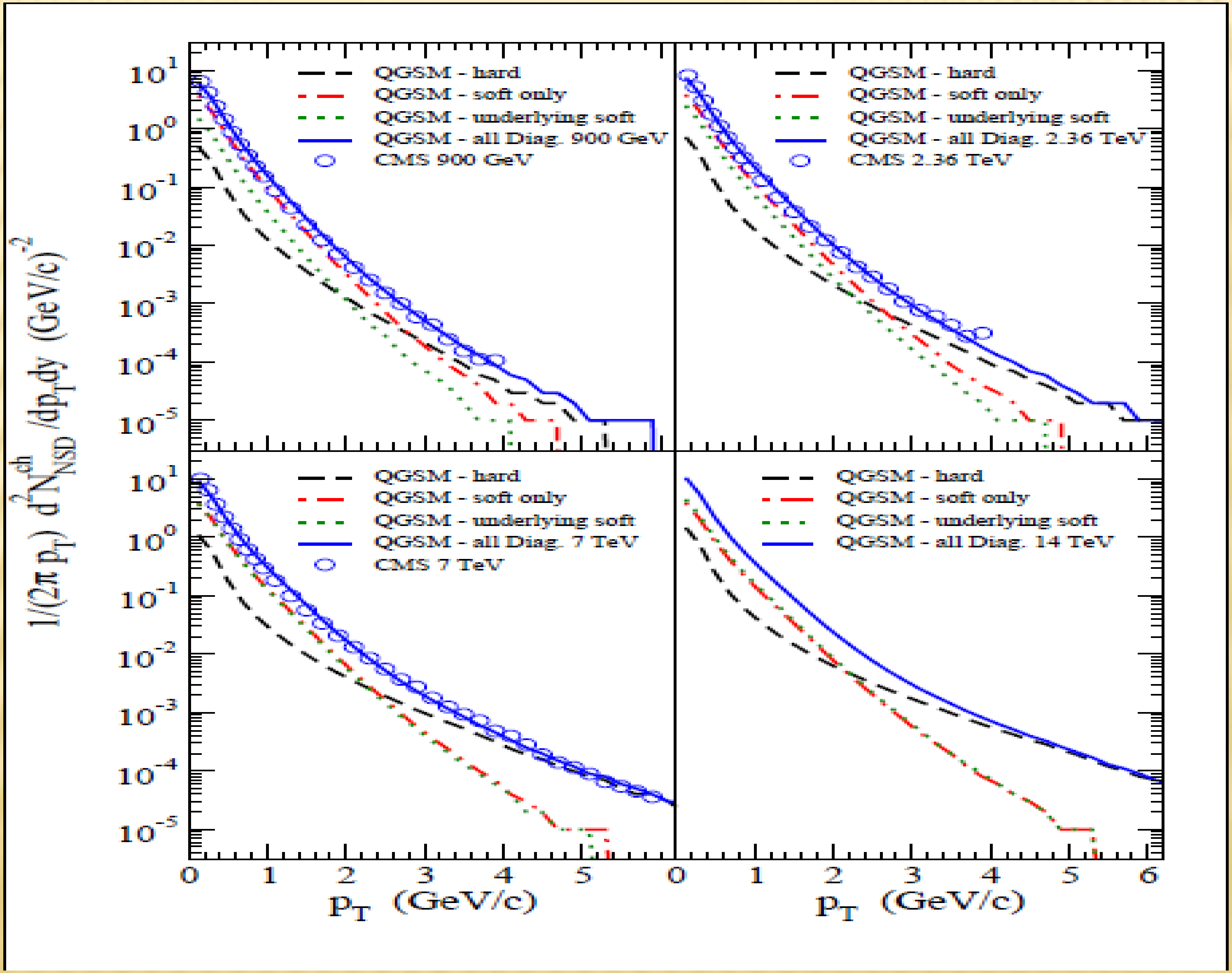

J.Bleibel, L.B. et al. (work in progress)

VIOLATION OF FEYNMAN SCALING

UA5 Collab., Phys. Rep. 154 (1987) 247

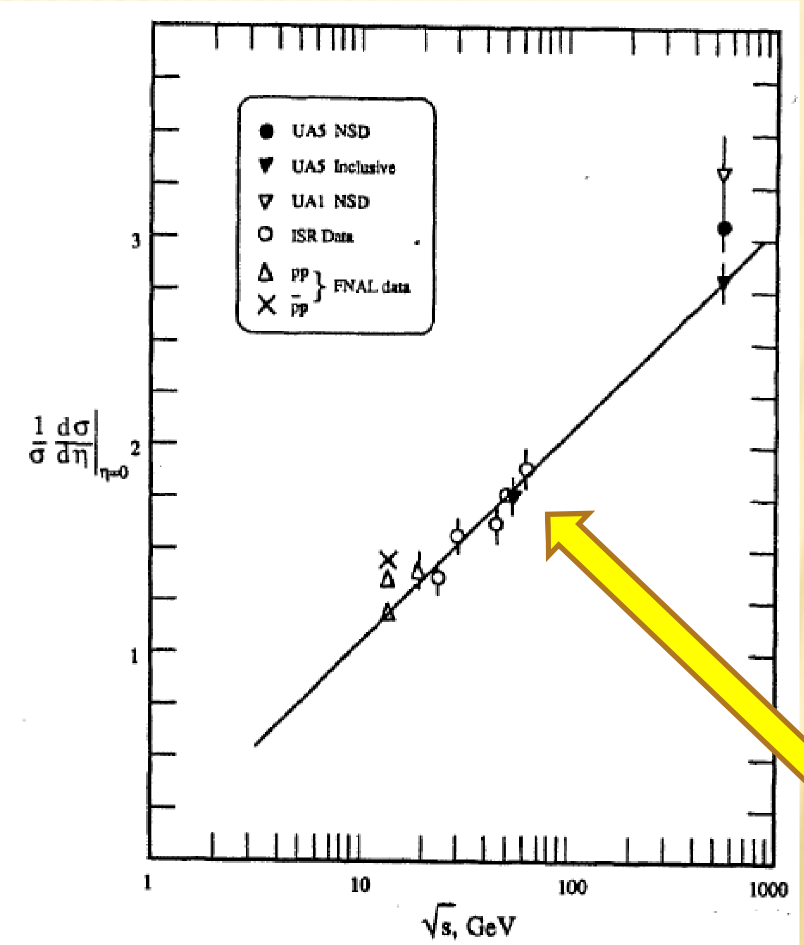

W. Busza, JPG 35 (2008) 044040

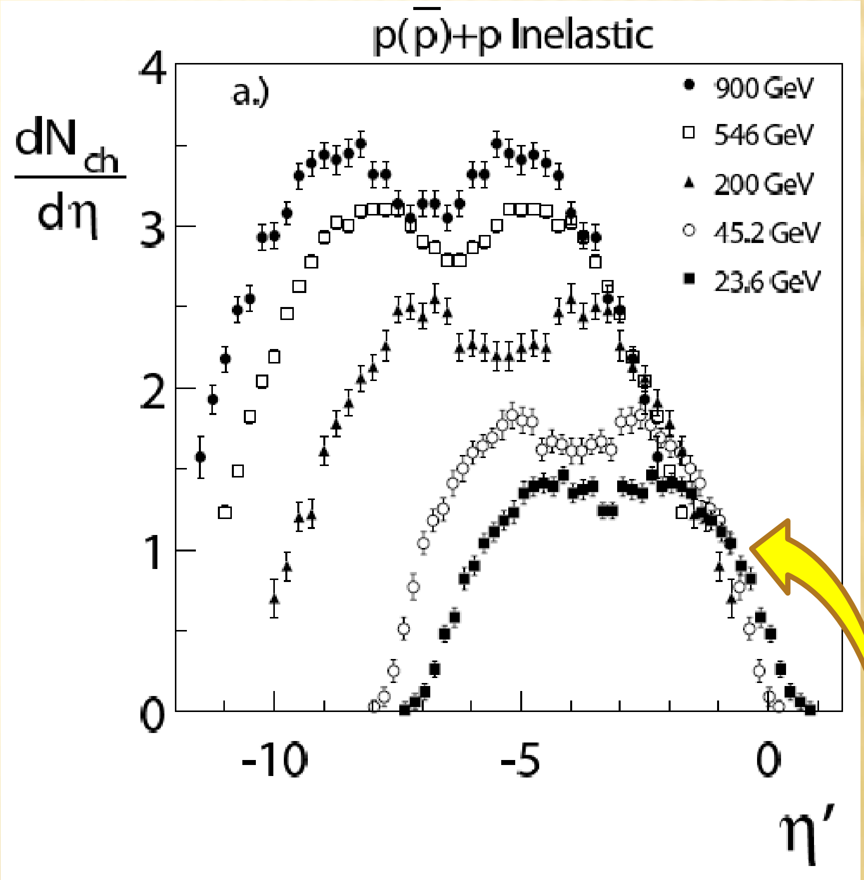

Charged particle pseudorapidity density at $\eta = 0$ as a function of $\sqrt{s}$

Violation of Feynman scaling, but ext. long. scaling holds?!

VIOLATION OF *Extended Longitudinal Scaling* IN HEAVY-ION COLLISIONS AT LHC?

J. Cleymans, J.Struempfer, L.Turko, PRC 78 (2008) 017901

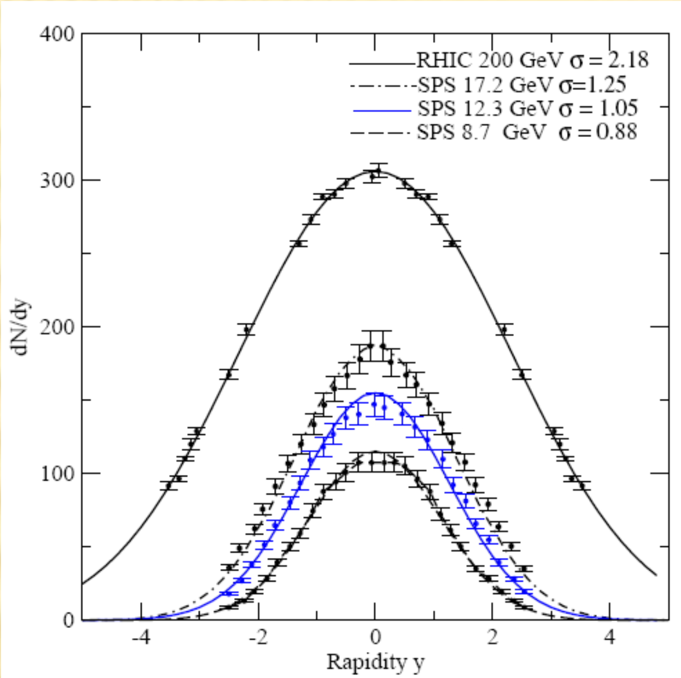

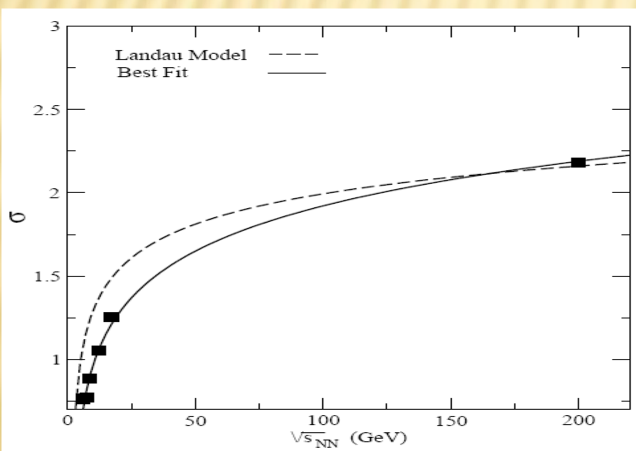

σ

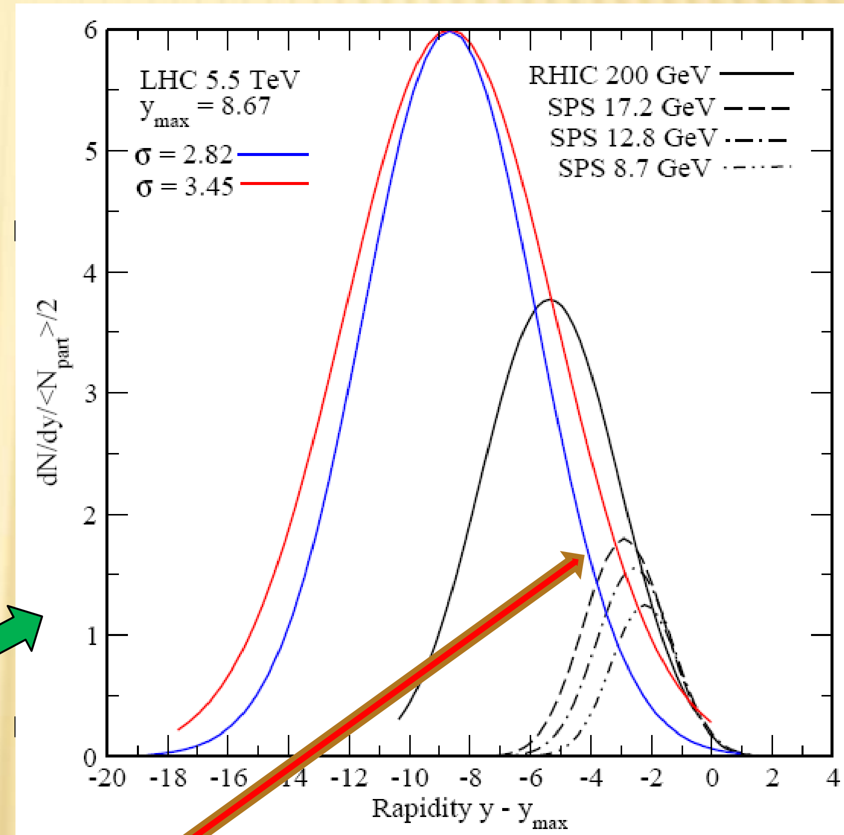

Statistical thermal model: ELS will be violated in A+A @ LHC. What about p+p ?

PREDICTIONS FOR PP @ LHC

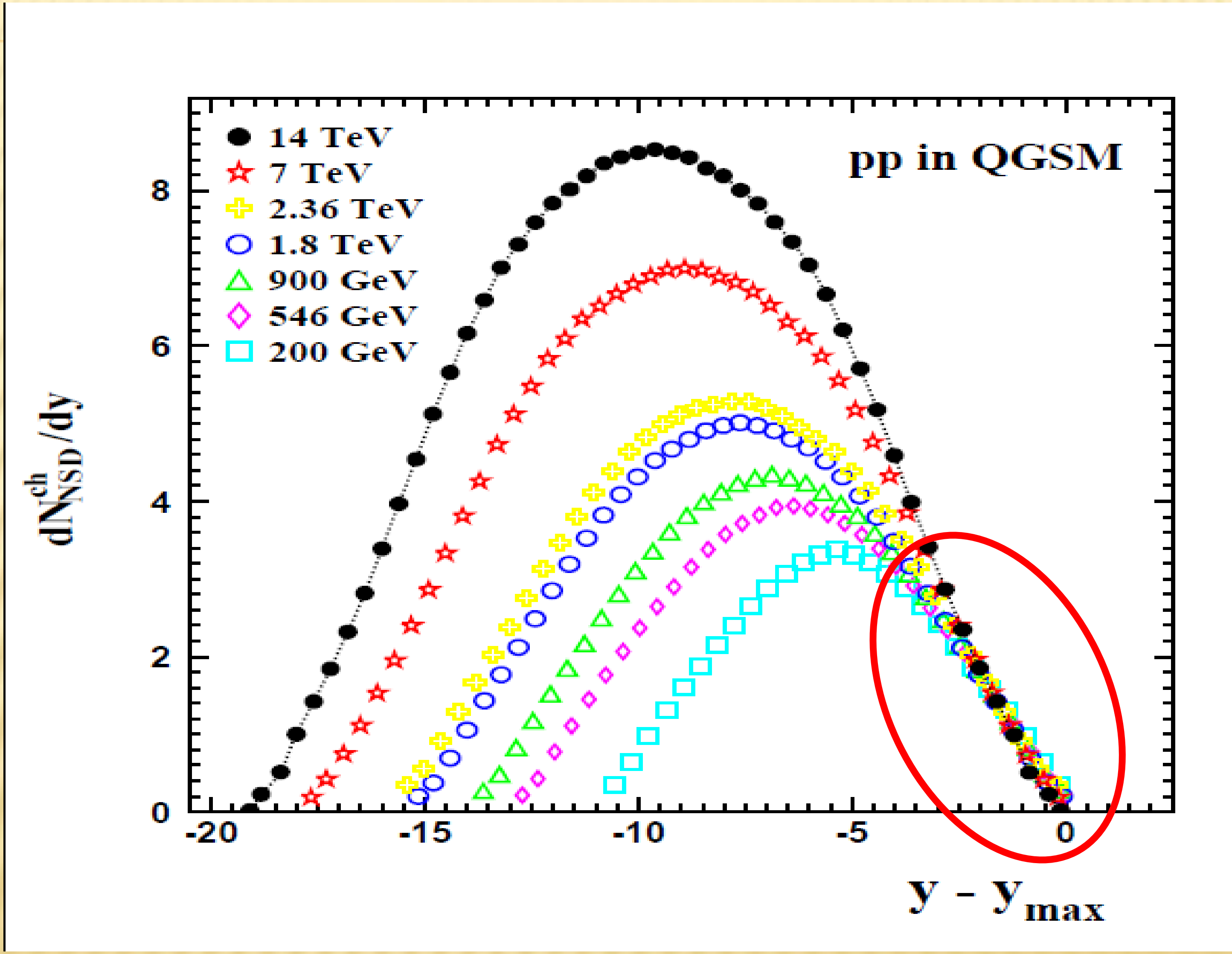

QGSM: extended longitudinal scaling in p+p collisions holds

WHY SCALING HOLDS IN THE MODEL?

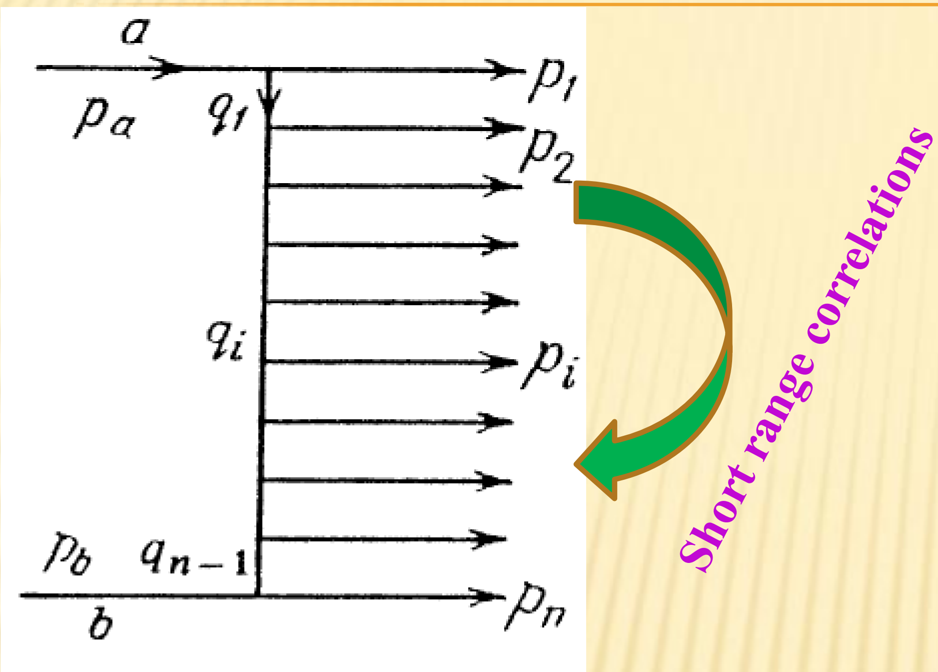

Correlation function

$$C(y_i, y_j) \propto \exp\{-\lambda(y_i - y_j)\}$$

Particles are uncorrelated if

$$y_i - y_j \equiv \Delta y \gg 1$$

Consider now inclusive process

$$1 + 2 \to i + X$$

Particle inclusive cross section

$$f_i = \frac{d^2\sigma(y_1 - y_i, y_i - y_2, p_{iT}^2)}{dy_i d^2 p_{iT}}$$

In the fragmentation region of particle 1

$$y_1 - y_i \approx 1,\; y_i - y_2 \approx y_1 - y_2 \gg 1$$

Inclusive density

$$\mathrm{n}_i = f_i / \sigma_{inel} = \phi(y_1 - y_i, p_{iT}^2)$$

$$x_F^{(i)} \equiv \frac{p_{i\|}}{p_\|^{\max}} \approx \exp\{-(y_1 - y_i)\}$$

therefore

$$n_i = \psi(x_F^{(i)}, p_{iT}^2)$$

In string models both FS and ELS holds in the fragmentation regions

QGSM PREDICTIONS and RESULTS FOR LHC

Multiplicity distributions

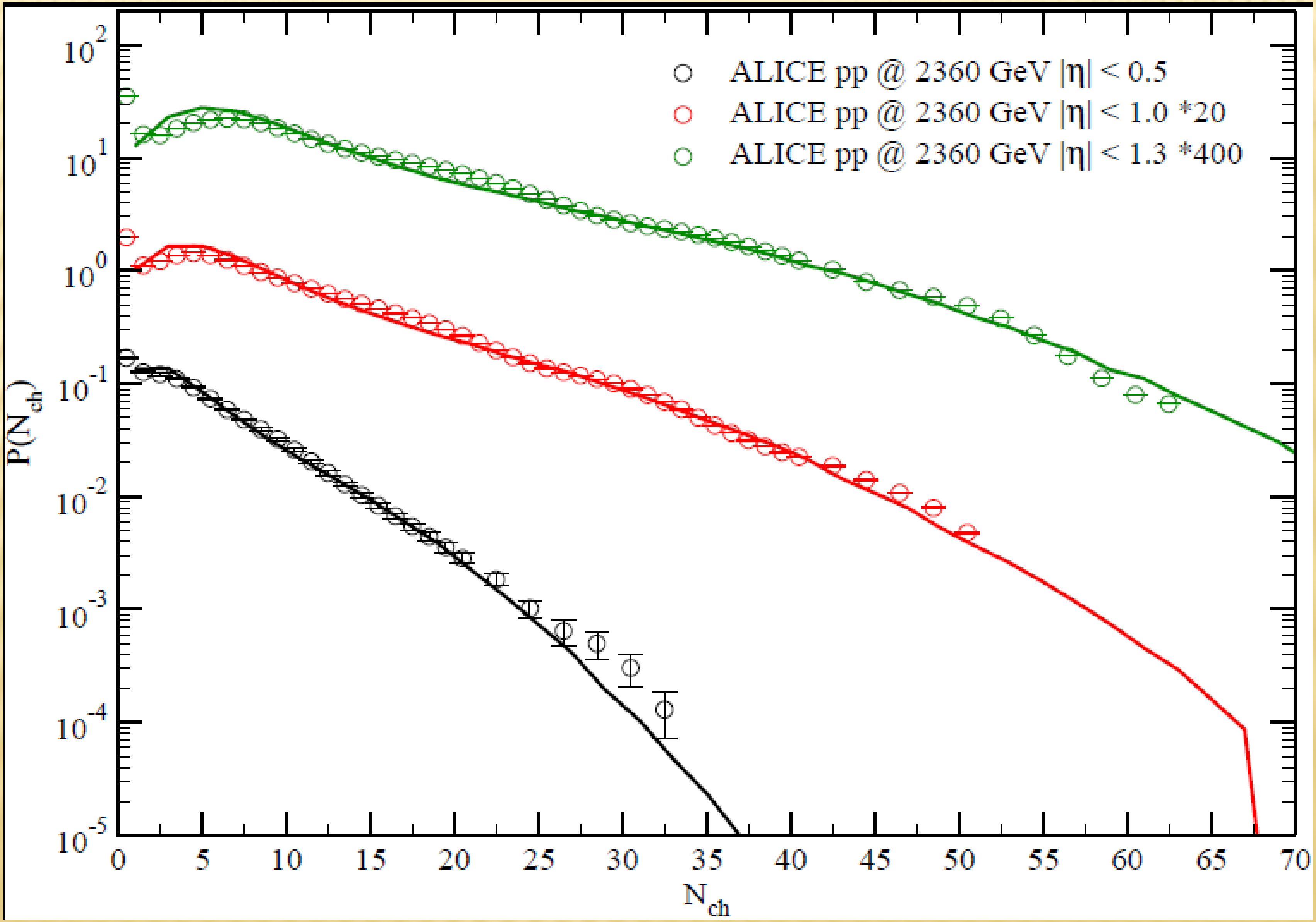

J.Bleibel, L.B. et al. (work in progress)

VIOLATION OF KNO SCALING AT LHC

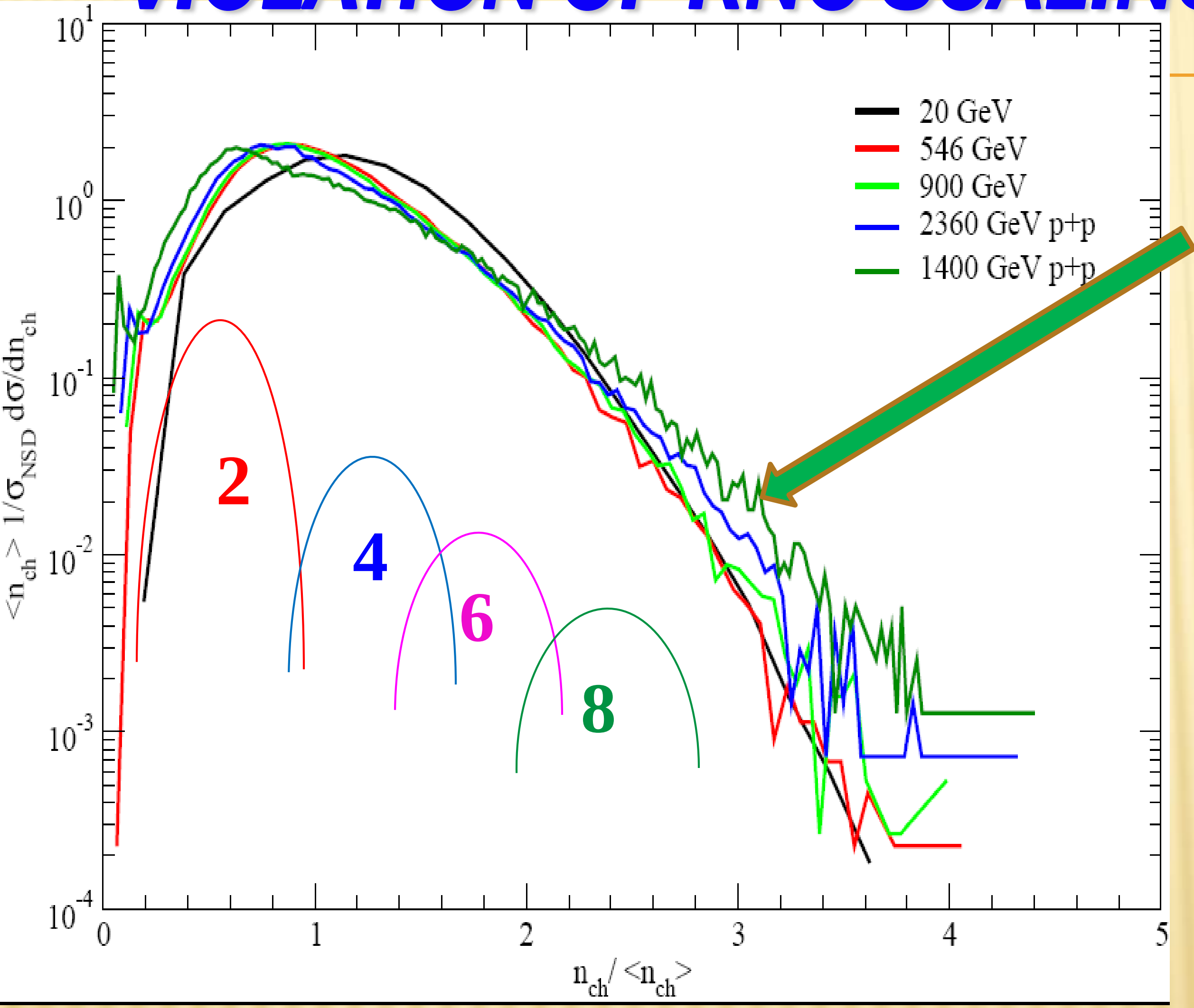

High-multiplicity tail is pushed up, whereas maximum of the distribution is shifted towards small values of z

At energies below 100 GeV different contributions overlap strongly, whereas at higher energies – more multi-string processes

=> Enhancement of high multiplicities

QGSM PREDICTIONS and RESULTS FOR LHC

Violation of KNO scaling at LHC

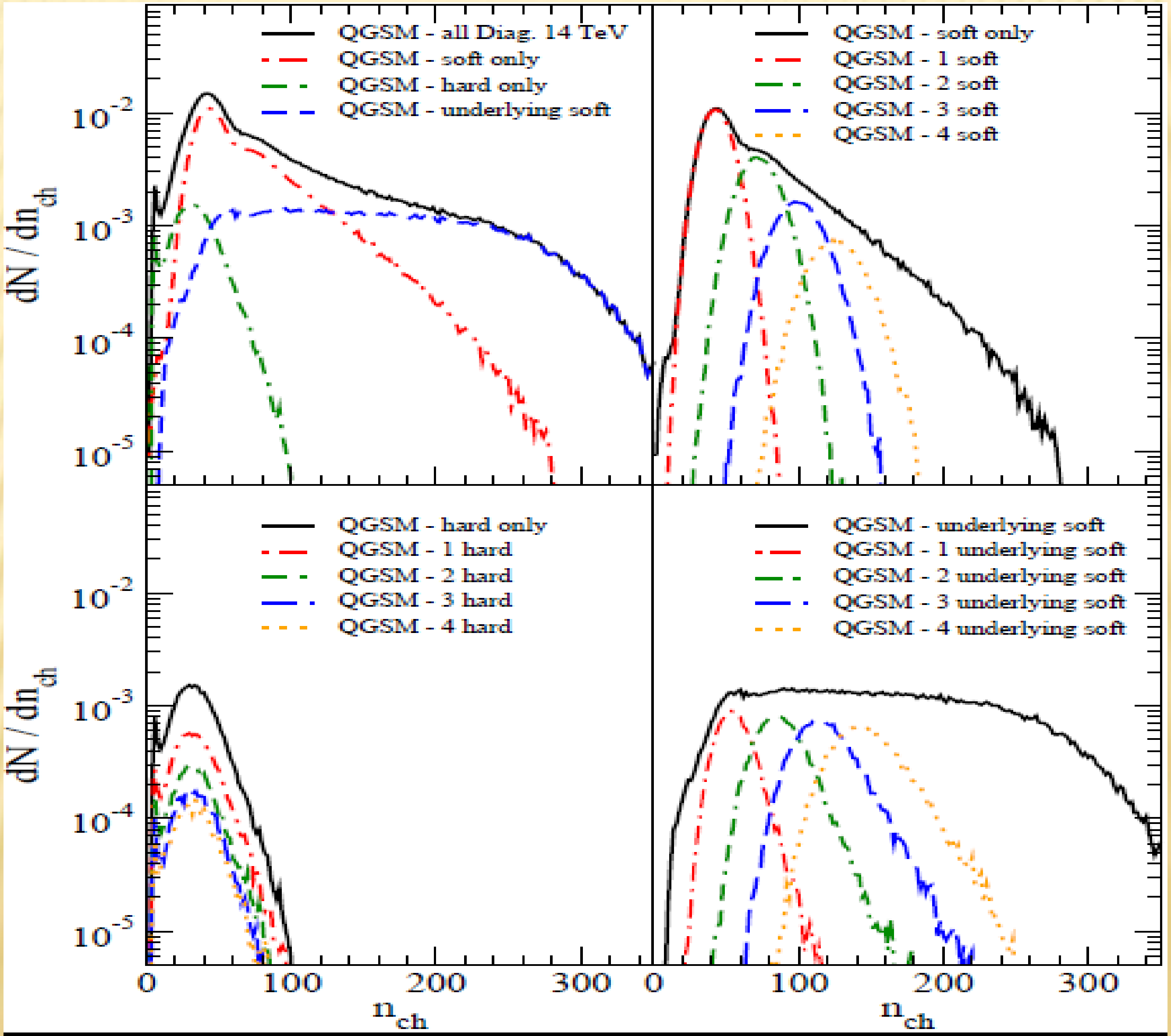

J.Bleibel, L.B. et al. (work in progress)

QGSM: Predictions for LHC. (14 TeV)

1.	$\sigma^{(tot)}$	103 mb	$(\sigma^{(tot)}(s) \sim \ln^2 \frac{s}{s_0})$
2.	$\sigma^{(el)}$	26 mb	$(\sigma^{(el)}(s) \sim \ln^2 \frac{s}{s_0})$
3.	$B(0)$	21.5 GeV^{-2}	$(B(0) \sim \ln^2 \frac{s}{s_0})$
4.	$\rho = \frac{Re T(0)}{Im T(0)}$	0.11	
5.	σ_{SD}	12÷13 mb	$(\sigma_{SD} \sim \sigma_{DD} \sim \ln \frac{s}{s_0})$
6.	σ_{DD}	11÷13 mb	

$$\sigma^{(el)} + \sigma_{SD} + \sigma_{DD} = 51\,mb \approx \frac{1}{2}\sigma^{(tot)}$$

QGSM: Predictions for LHC.

7. $\langle n_{ch} \rangle$ $\quad 80 \div 100$

8. $\left.\frac{dn_{ch}}{dy}\right|_{y=0}$ $\quad 5.5 \div 6.0$

9. Structures in σ_n

10. Strong long-range (in y) correlations

11. Large amount of minijets.

QGSM gives a unified description of:

$$\sigma^{(tot)}{}_{hp}(s), \quad \frac{d\sigma^{(el)}}{dt}, \quad E\frac{d^3\sigma}{d^3p}$$

for $\pi^{\pm}, K^{\pm}, K^0(\bar{K}^0), p, \bar{p}, \Lambda, \bar{\Lambda}, ..$

$\sigma_n(s)$, correlations,…

Substantial deviations from predictions of the model at superhigh energies would indicate to a new physics.

3.HANBURY-BROWN—TWISS CORRELATIONS

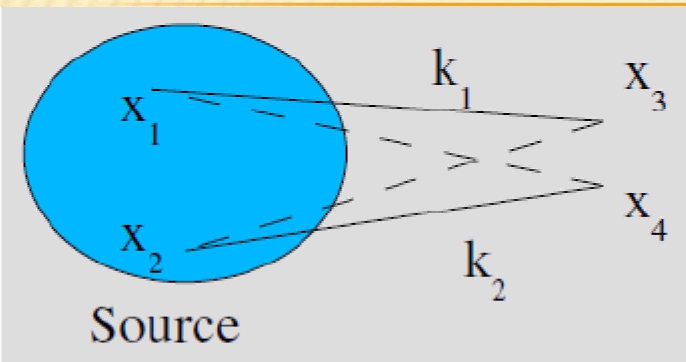

$$\mathbf{q} = \mathbf{p_1} - \mathbf{p_2}$$

- We can consider two pions emitted from two spacetime points in the extended source.
- Correlations will then arise from exchange symmetry between identical particles.
- It is defined as the probability to measure both particles in coincidence, divided on the probability of measuring each separately.

$$C_2(k_1, k_2) = \frac{P(k_1, k_2)}{P(k_1)P(k_2)}$$

$$C_2(q) = 1 + \lambda e^{-R_{out}^2 q_{out}^2 - R_{side}^2 q_{side}^2 - R_{long}^2 q_{long}^2 - R_{out,long}^2 q_{out,long}}$$

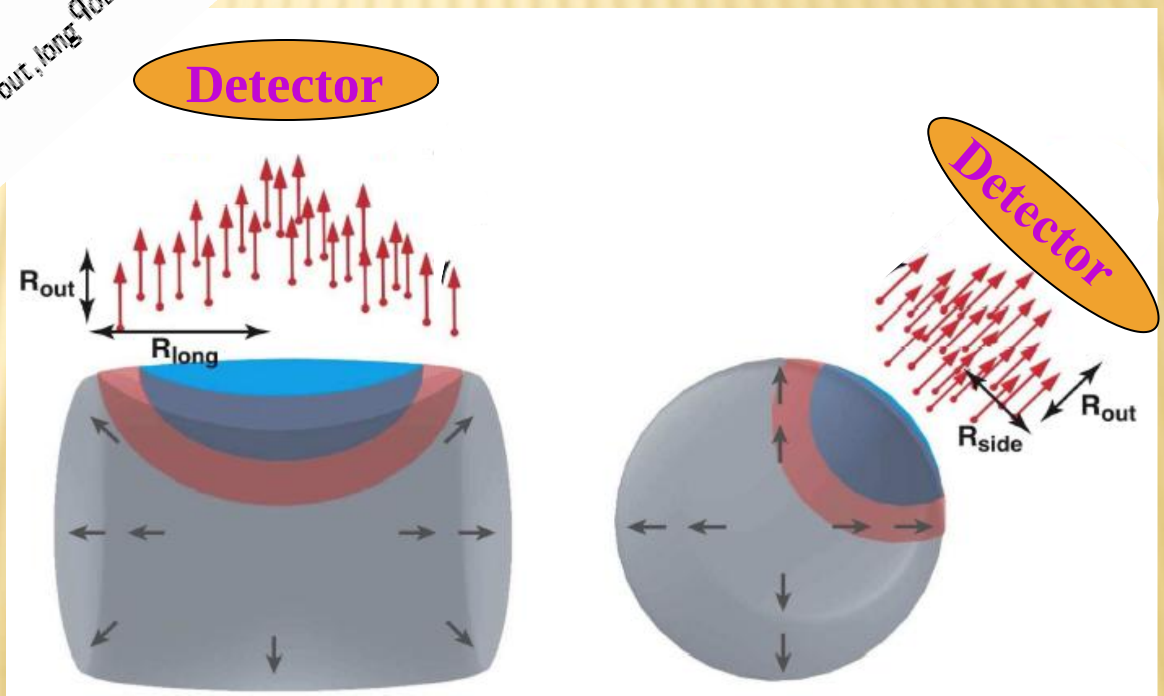

Comparison to experimental data

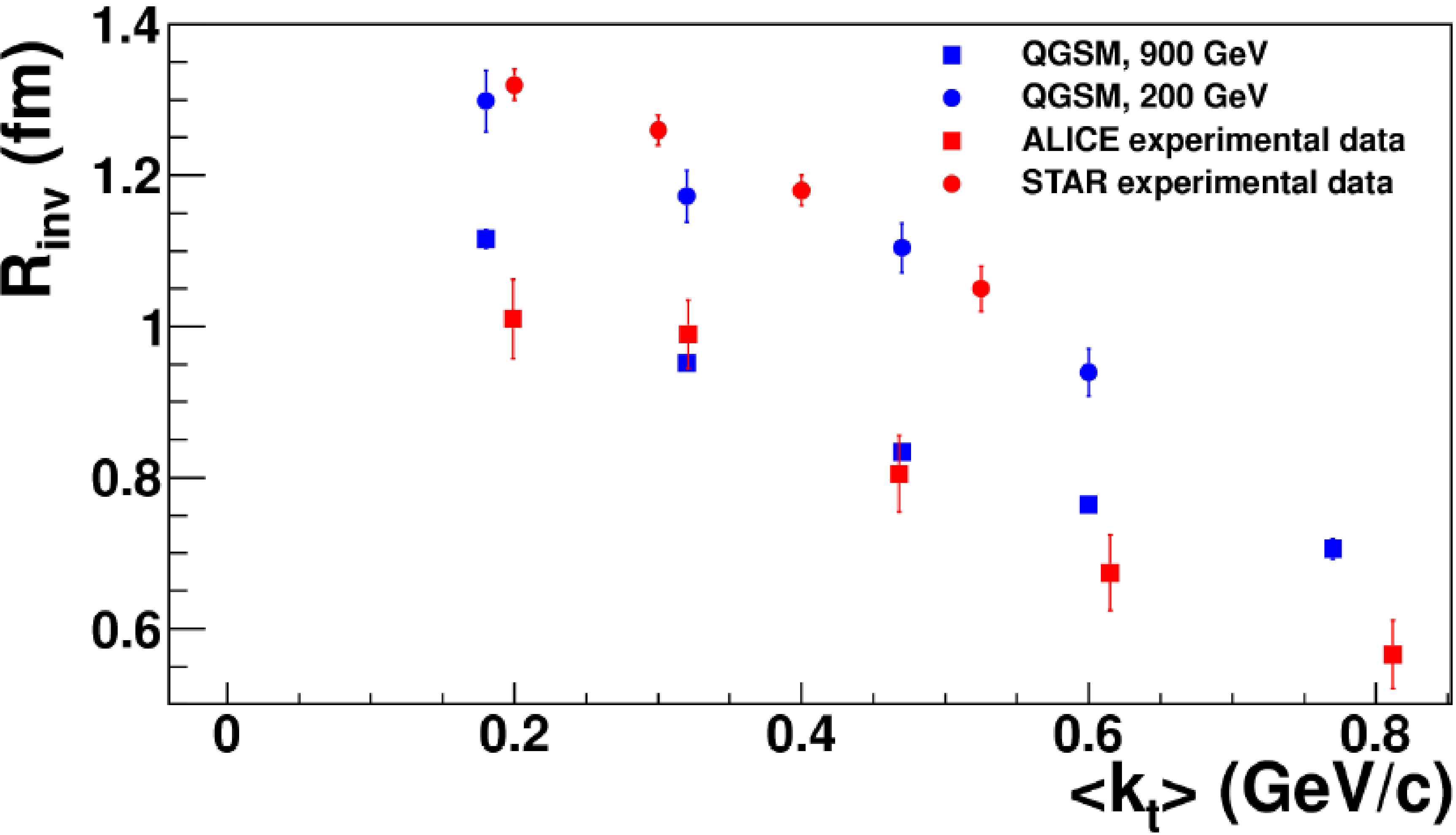

Correlation radii 200GeV

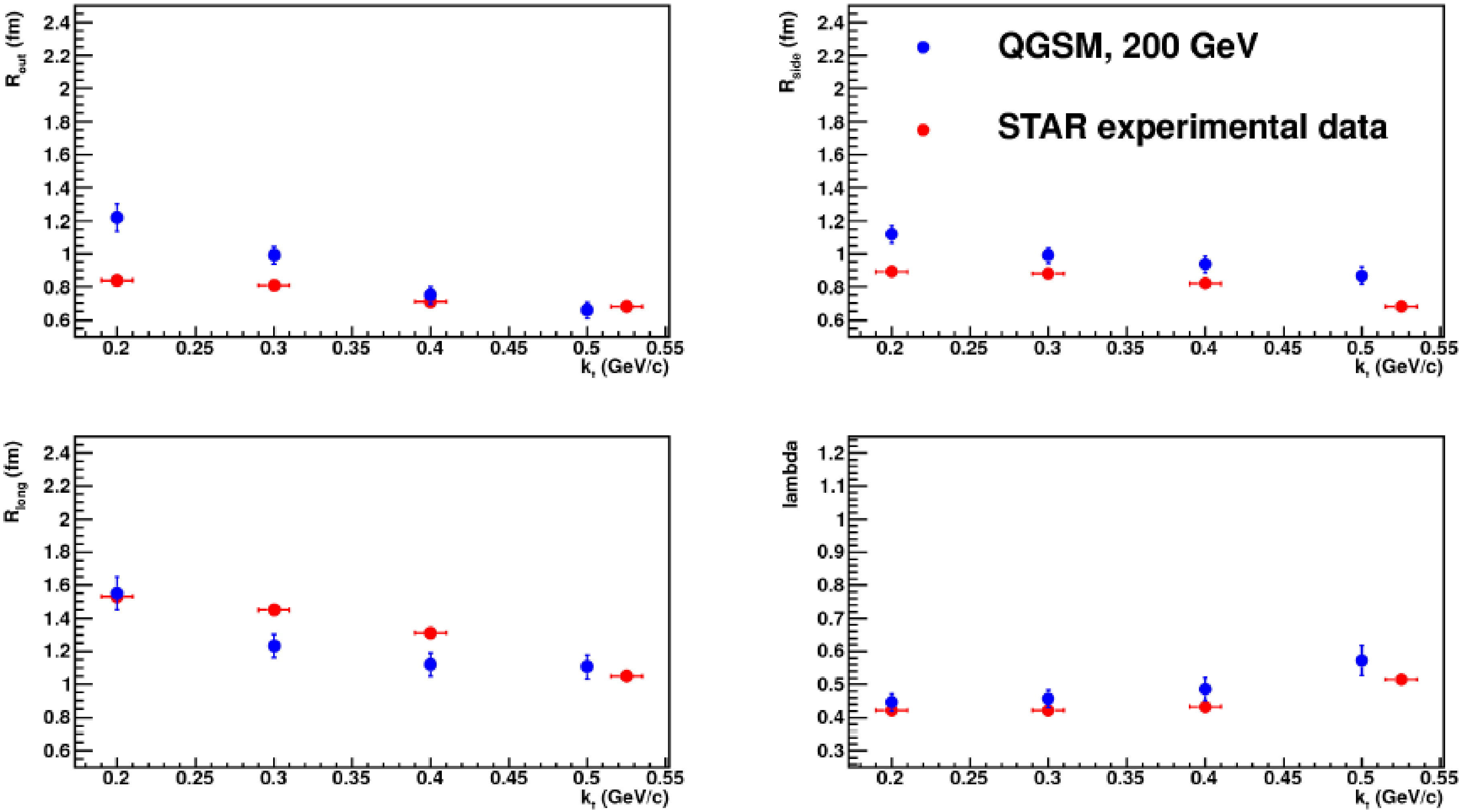

Correlation radii 900 GeV

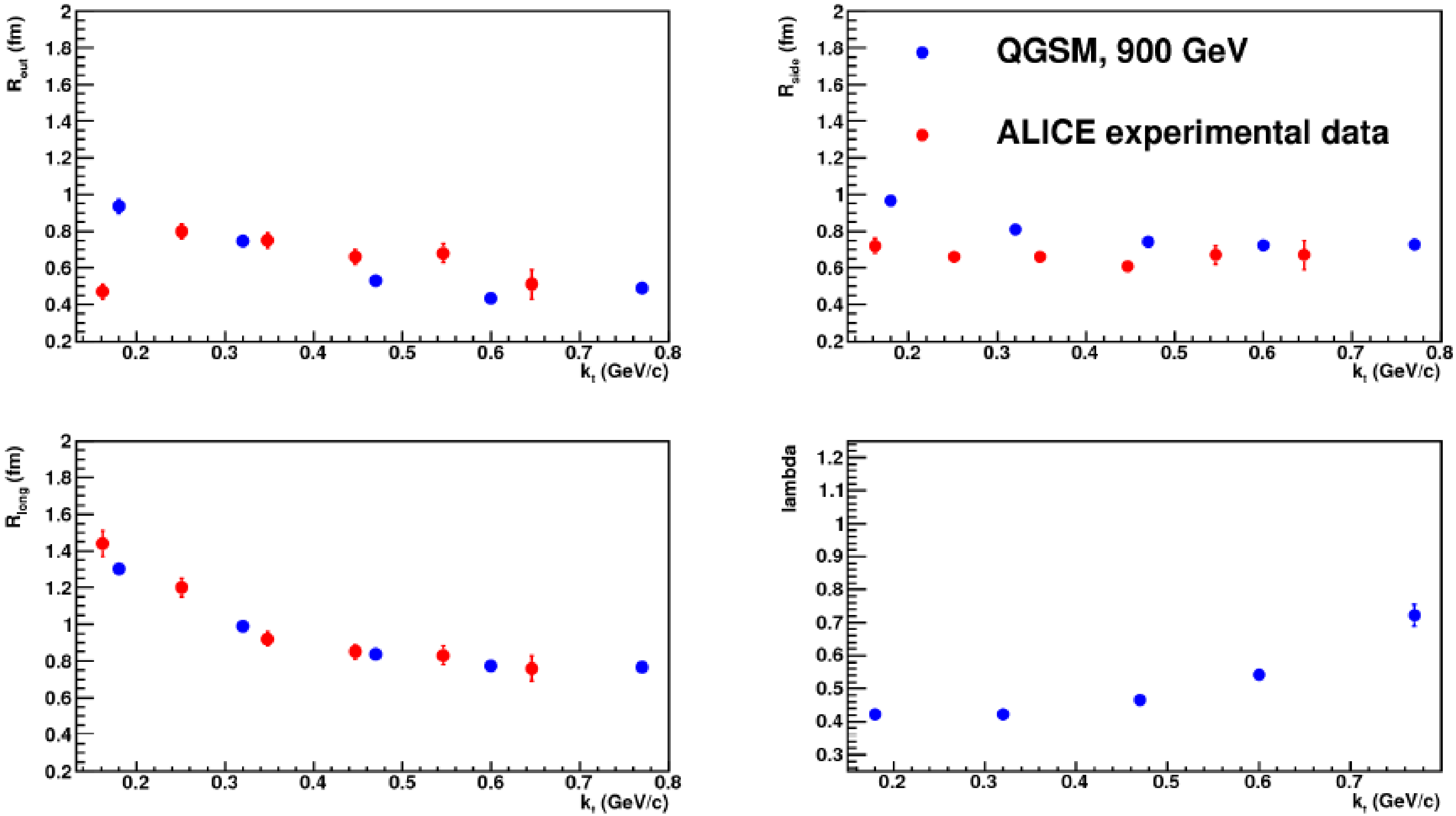

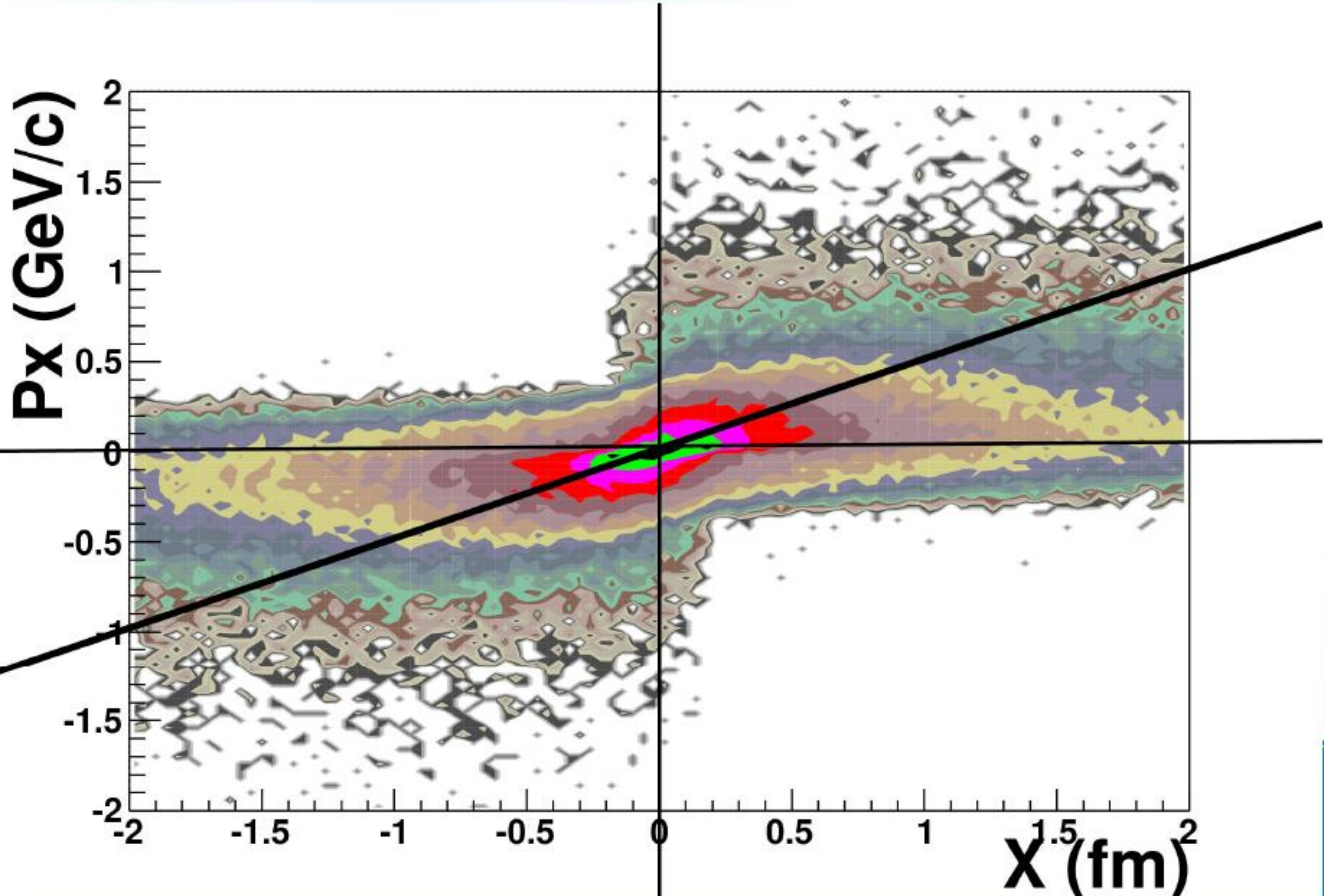

Px (GeV/c)
2
1.5
1
0.5
0
-0.5
-1
-1.5
-2
-2
-1.5
-1
-0.5
0
0.5
1
1.5
2
X (fm)

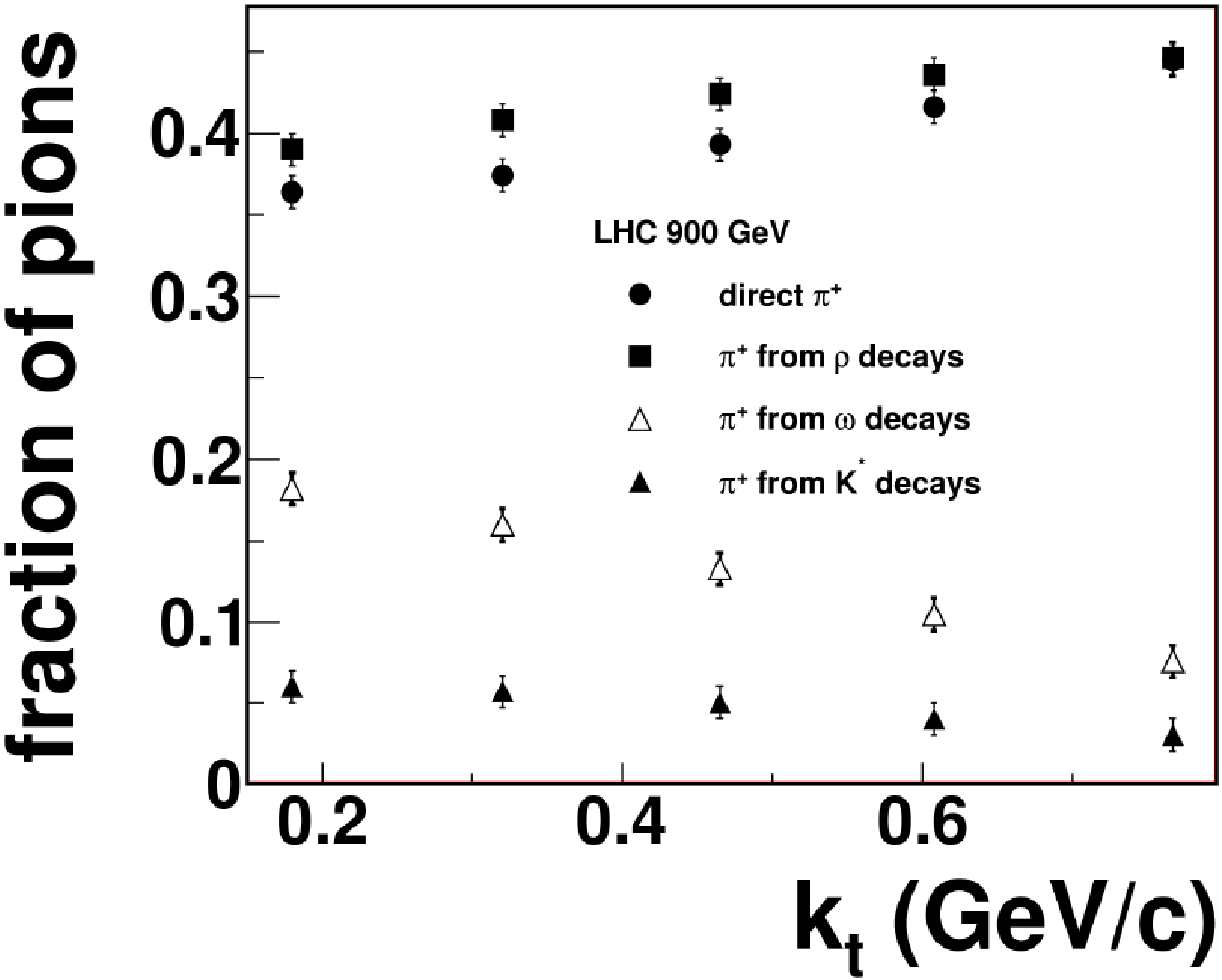
fraction of pions
0.4
0.3
0.2
0.1
0
0.2
0.4
0.6
k_t (GeV/c)
LHC 900 GeV
direct π⁺
π⁺ from ρ decays
π⁺ from ω decays
π⁺ from K* decays

4. Anisotropic flow in pp

Azimuthal anisotropy in relativistic string fragmentation, I

Accepted picture for flow in heavy ion collisions – hydro expansion of QGP. Still, flow in *pp* and light AA is an open question:

- ? possible reasons for it
- ? magnitude
- ? possibility of observation

All the points are linked with each other

$\Rightarrow$ Importance of models as a test-ground for study of possible mechanisms.

Possibility of flow in DPM

- DPM: final particles come as fragments of *qg* strings, *N* of strings is defined via RFT.
- RFT study (K.Boreskov, A.Kaidalov, O.Kancheli) proposes asimuthal anisotropy.
- Model for $\mathbb{P}$ with transverse separation of its ends – *qg* string $\longrightarrow$ relativistic string with transverse separation of its ends.

Status of anisotropic flow in AA (and in pp)

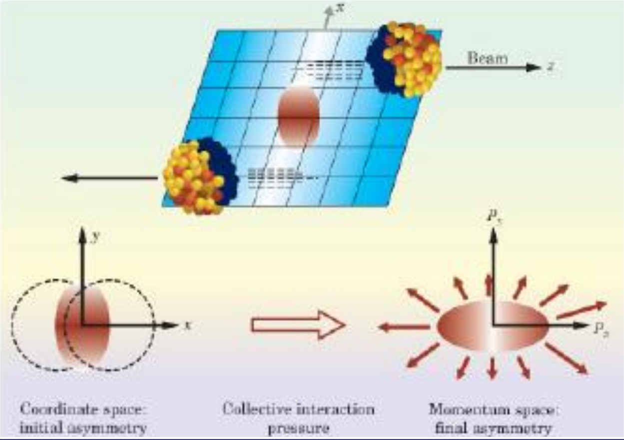

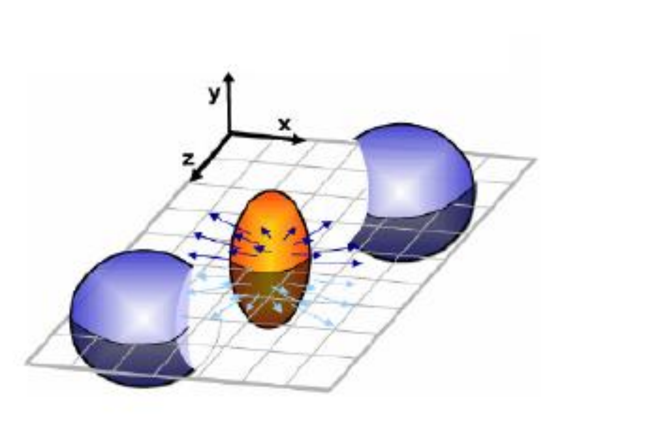

Ollitrault's suggestion (1992):

Finite impact parameter collisions => *anisotropic spatial density.*
Unequal pressure gradients (assuming thermalisation) produces an *anisotropic momentum distribution* of particles.

The strength of the anisotropy, and its systematic dependence on various parameters, provides *information on the equation of state*.

$$\frac{d^3N}{dp_t\, dy\, d\varphi} \propto 1 + 2v_1 \cos(\varphi) + 2v_2 \cos(2\varphi) + \ldots$$

Directed flow (v_1) — Elliptic flow (v_2)

$$v_2 = \left\langle \frac{p_x^2 - p_y^2}{p_x^2 + p_y^2} \right\rangle = \langle \cos(2\phi) \rangle$$

Fourie expansion of invariant cross section:

Results on anisotropic flow in AA

it depends on – energy, centrality,rapidity, pt, particle id:

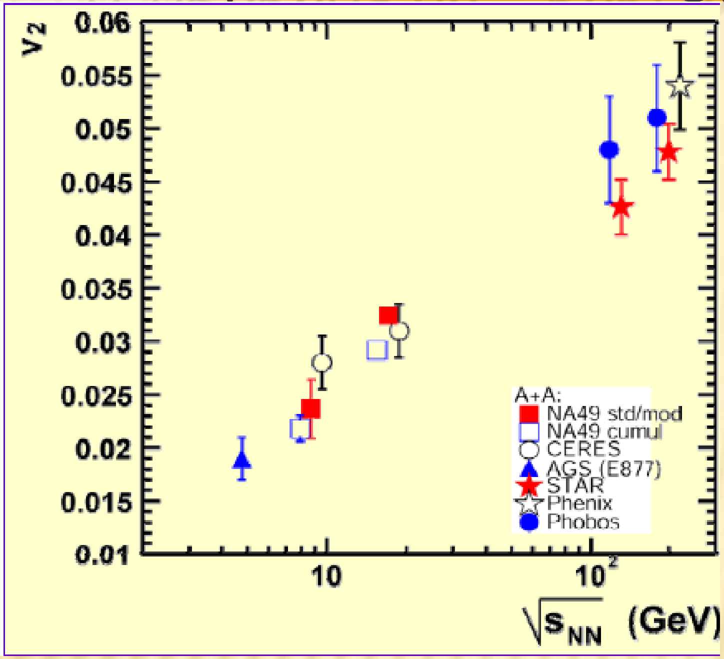

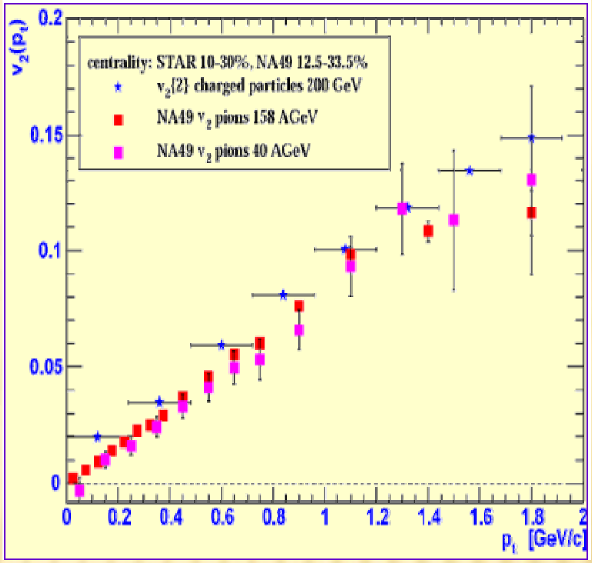

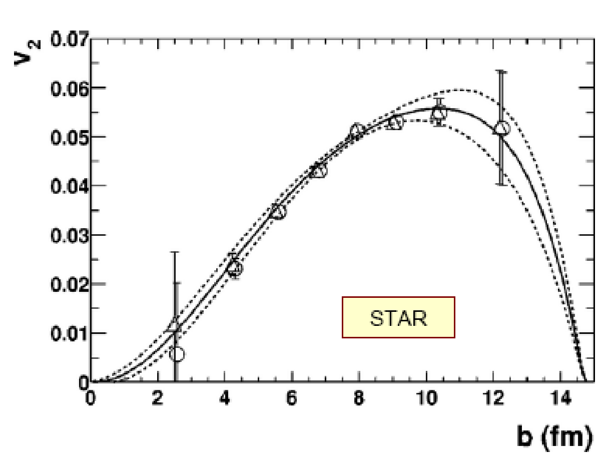

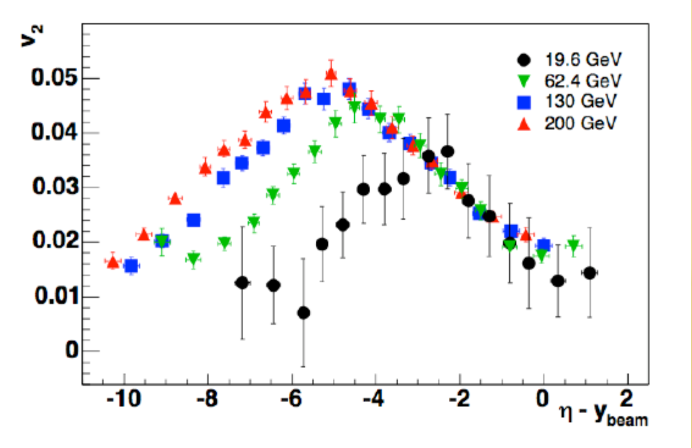

Anisotropic flow in pp

Estimates of hadron azimuthal anisotropy from multiparton interactions in proton-proton collisions at sqrt(s) = 14 TeV. D. d'Enterria , G.Kh. Eyyubova, et al Eur.Phys.J.C66:173,2010.

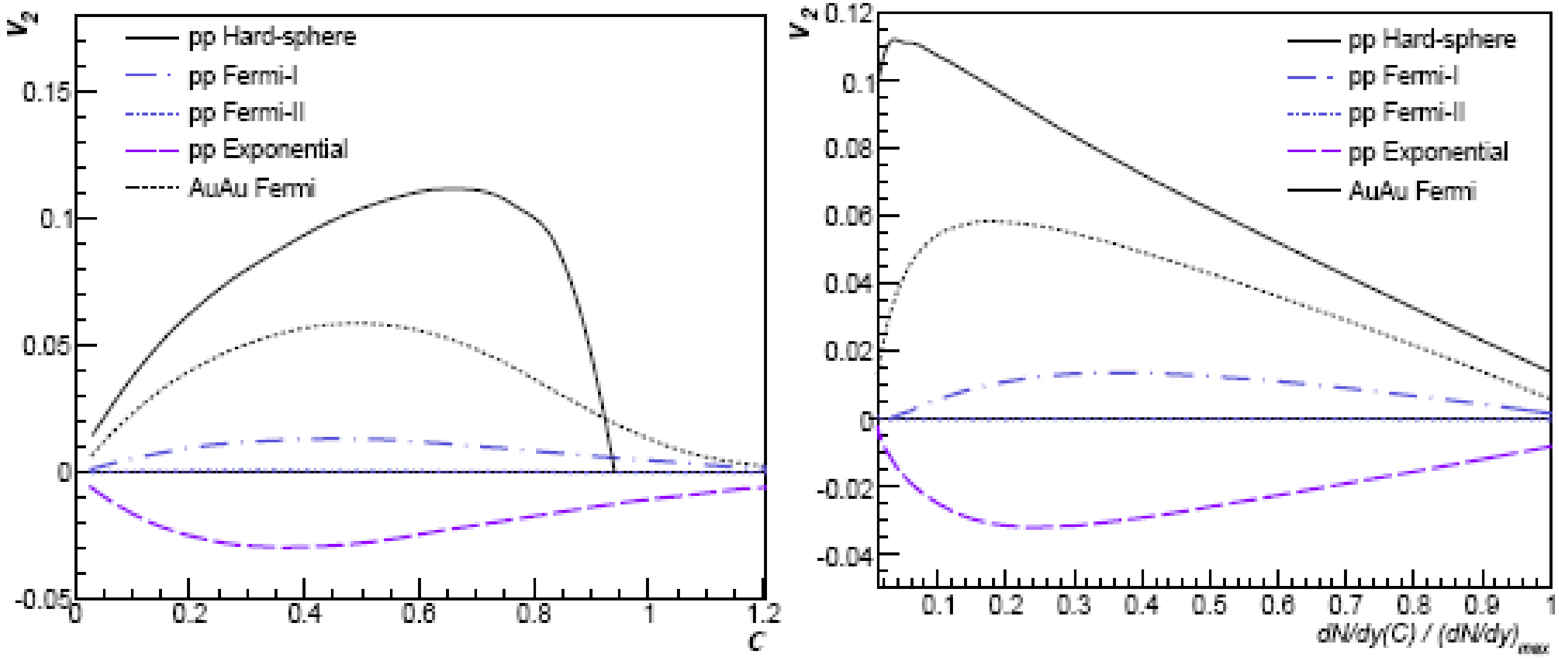

Fig. 8. Integrated elliptic flow v_2 parameter as function of centrality (left panel) and of normalised particle multiplicity (right panel) at midrapidity in *p-p* collisions at $\sqrt{s}$ = 14 TeV for the different proton density distributions considered in this work (Table 1). For comparison, the v_2 for *Au-Au* at RHIC energies is shown as a dotted line.

ANISOTROPIC FLOW IN PP

Anisotropic flows from initial state of a fast nucleus.
K.G. Boreskov, A.B. Kaidalov, O.V. Kancheli, Eur.Phys.J.C58:445-453,2008.

In Regge theory it appears as initial state effect and inversely proportional to the radius of the object: for pp it could be larger then for AA :

$$\Gamma(\vec{a},\vec{p}_t) \propto [1+\varepsilon p_{t,i} p_{t,j}\, \partial_i \partial_j]\delta^{(2)}(\vec{a})$$

Elliptic flow

$$v_2 = \varepsilon \frac{r_0^4\, T''_{overlap}(b^2)}{T_{overlap}}\left(r_0^2 p_t^2\right) = \frac{\varepsilon}{16}\frac{r_0^2}{R_A^2}\frac{b^2}{R_A^2}\left(r_0^2 p_t^2\right)$$

$$T_{overlap} = T_1 \otimes T_2$$

In Gauss approximation

Оценка:

$$A \sim 200;\ \ p_t \sim 1\ GeV/c;\ \ b \sim R_A;$$
$$r_0 / R_A \sim 1/6;\quad r_0 p_t \sim 5$$

$$v_2 \sim 0.05\varepsilon$$

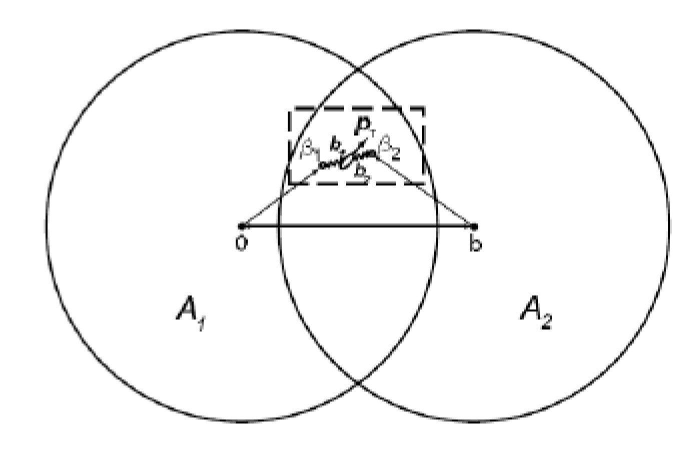

Anisotropic flow in pp

Azimuthal anisotropy in relativistic string fragmentation, II

Comparatively simple model, only one sort of particles("π-mesons").

But: explicitly observed string dynamics;
explicit energy-momentum conservation.

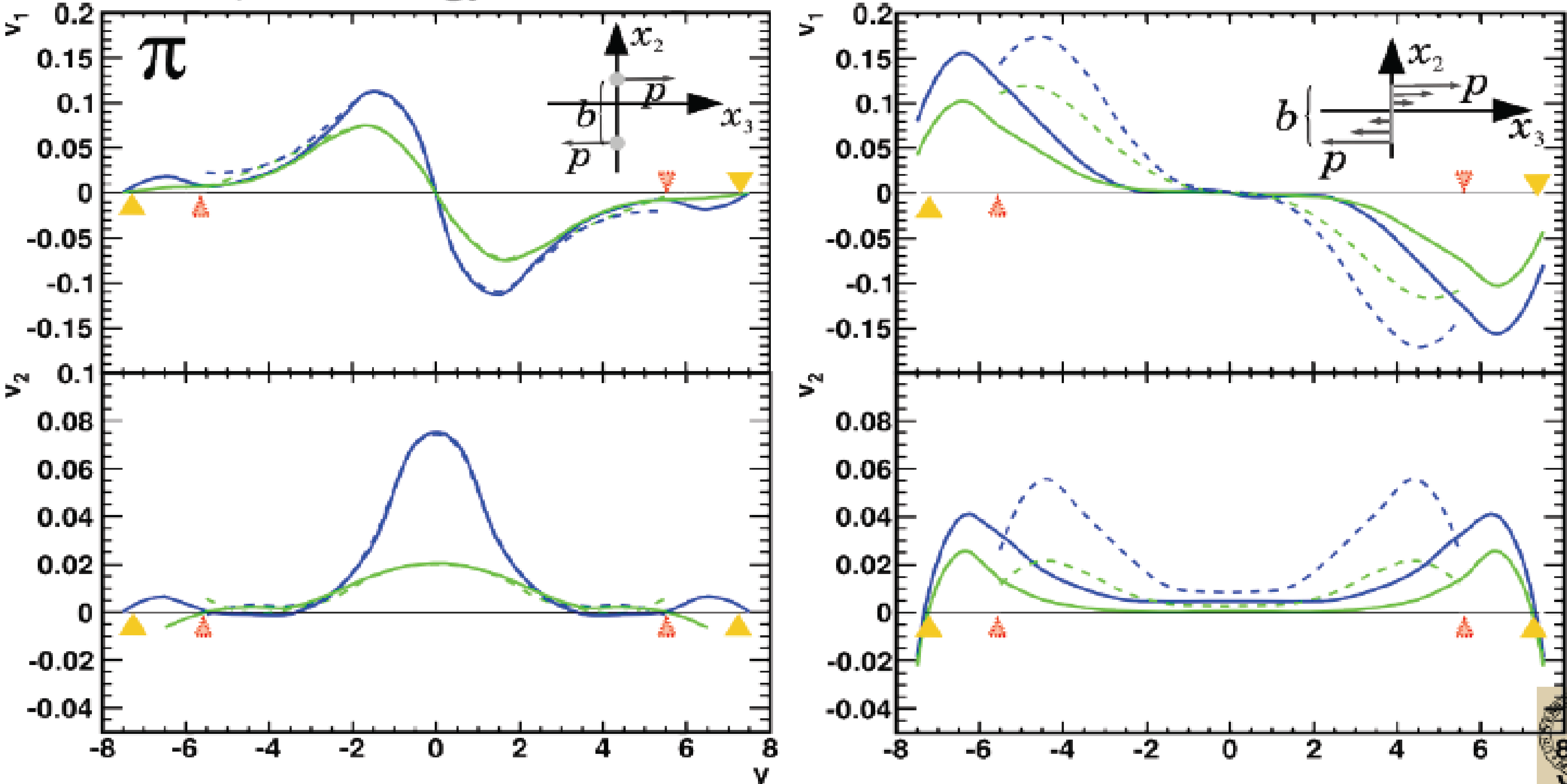

b = 0.5 fm ▬, 1 fm ▬; s^1/2 = 40 GeV, 200 GeV.

Anisotropic flow in pp

Azimuthal anisotropy in relativistic string fragmentation, III

RESULTS:

1. Both v_1 and v_2 present; positive v_2, v_1 comes with the same sign as v_1 in AuAu experiment.
2. Extreme sensitivity to the internal momentum distribution.

Paper R.Kolevatov "On azimuthal anisotropy in fragmentation of classical relativistic string " (arXiv:0912.5377v1 [hep-ph]);

Eur.Phys.J. C68 (2010) 513-521

OUTLOOK:

1. Application to pp involve $2 \times n$ strings asymmetric in rapidity,
2. Need much deeper understanding of string formation within RFT (see p.2 of the results)

Summary and outlook

- LHC is a discovery machine for both hard and soft physics in HI collisions
- Event generators are an indispensable tool for planing the experiments and analysis of data
- => Further development of existing MC generators
- HI theory groups in Oslo utilizes it to study :
  EOS, elliptic flow, particle freeze-out, HBT correlations of unlike particles, particle-jet correlations, heavy quark production in a large pT range, scaling properties …

MANY THANKS TO OAC FOR HOSPITALITY!!!

I.Alsybeev, G.Feofilov, A.Ivanov, V.Vechernin
SAINT-PETERSBURG STATE UNIVERSITY

Motivation(theory) Application of string model.

Investigations of the charged particles long-range multiplicity correlations, measured for well separated rapidity intervals, can give us information on the number of emitting centers and hence on the fusion of color strings[2,3].

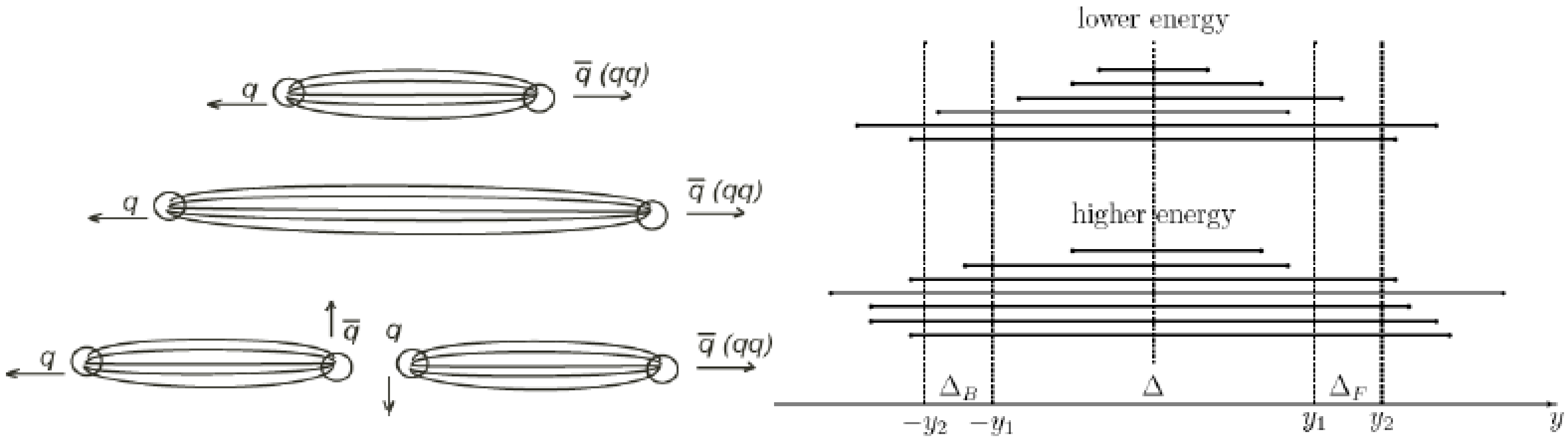

Fig.1. Quark-gluon strings and schematics for studies of Long-Range Correlations[2]

A.B.Kaidalov, Phys. Lett., **116B**(1982)459;
A.B.Kaidalov K.A.Ter-Martirosyan, Phys.Lett., **117B**(1982)247.
A.Capella, U.P.Sukhatme, C.--I.Tan and J.Tran Thanh Van, Phys. Lett. **B81** (1979) 68; Phys. Rep. 236 (1994) 225.
Abramovskii V. A., Gedalin E. V., Gurvich E. G., Kancheli O. V. , Long-range azimuthal correlations in multiple-production processes at high energies, JETP Lett., vol.47, 337-339 , 1988
M.A.Braun, C.Pajares and V.V.Vechernin, Low pT Distributions in the Central Region and the Fusion of Colour Strings, Internal Note/FMD ALICE-INT-2001-16

String fusion, centrality and low pt limit…

- Long-range part of multiplicity-multiplicity correlations in ALICE pp@7TeV is well described in the model with independent emitters (strings) but also we see nontrivial long-range Pt-Pt correlations that, in a field of string fusion model, require presence of string interaction.
- This means that in some events there are some emitters (string clusters) that have higher average Pt
- From this point of view "two main conditions to see near-side structure" means:
  1. **Centrality -** transverse string density must be sufficient to form string clusters with reasonable probability
  2. **Low Pt limit –** Low Pt limit (~0.8) rather high but it is still a soft process region. Such cut on Pt distribution can be a way to maximize contamination of particles coming form string clusters (sources having higher <Pt> than normal strings) in correlation function.

  Only combination of these two factors make near-side ridge structure visible.
- PtPt correlation is more sensible to string fusion effect than NN, so we are looking for a way to include Pt of both particles into $\Delta\eta$-$\Delta\varphi$ correlation function.

INTERPRETATION OF RIDGE IN PP

Physics of the ridge

Jet-Jet or Jet-proton remnant:
- Many questions about the role of jets
- Should predict ridge is always aligned with jet in ϕ

Hydrodynamic flow:
- Original motivation of the analysis
- Possible although degree of thermalization is hard to evaluate

Glasma tube from BNL group
- Glasma tube+radial flow -> ridge in HI
- Intrinsic ridge in pp even without radial flow
- Similar p_T dependence as the data

Wei Li, Oct 4, 2010, CMS QCD meeting

8. ANISOTROPIC FLOW IN PP

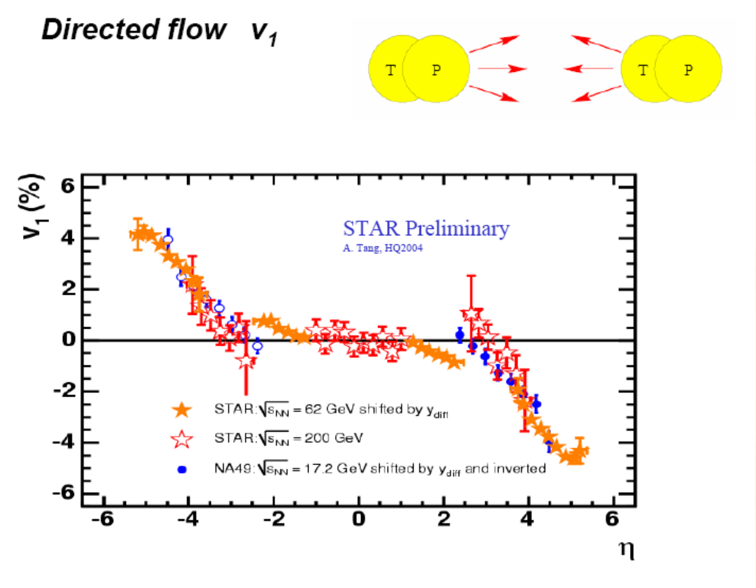

And connected with EOS and final state interactions.

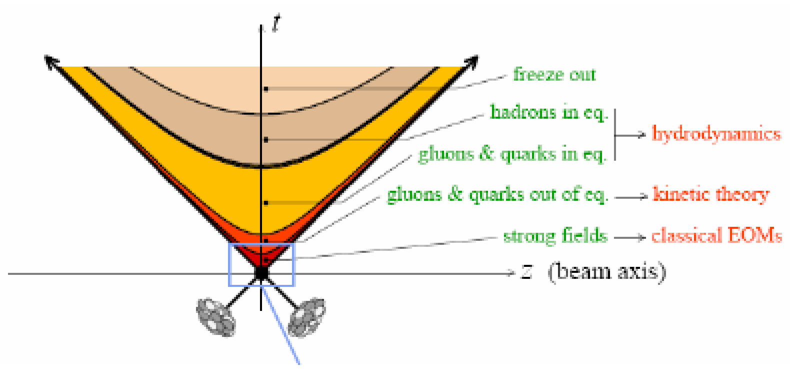

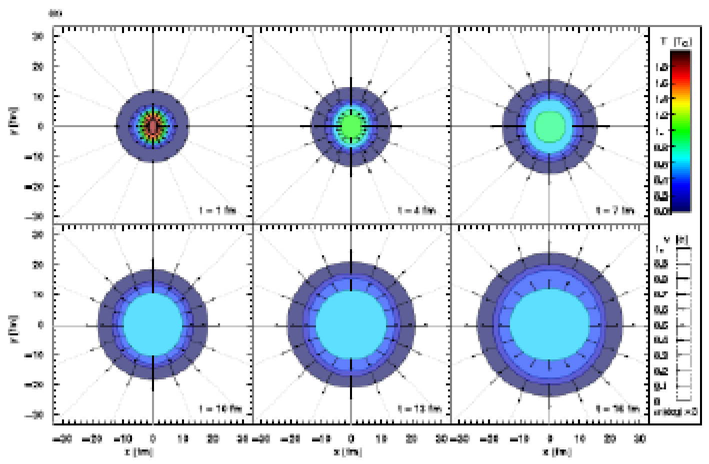

JET QUENCHING AT LHC?

arXiv:1011.6182v1 [hep-ex] 29 Nov 2010

Observation of a Centrality-Dependent Dijet Asymmetry in Lead-Lead Collisions at $\sqrt{s_{NN}} = 2.76$ TeV with the ATLAS Detector at the LHC

G. Aad *et al.* (The ATLAS Collaboration)*

Using the ATLAS detector, observations have been made of a centrality-dependent dijet asymmetry in the collisions of lead ions at the Large Hadron Collider. In a sample of lead-lead events with a per-nucleon center of mass energy of 2.76 TeV, selected with a minimum bias trigger, jets are reconstructed in fine-grained, longitudinally-segmented electromagnetic and hadronic calorimeters. The underlying event is measured and subtracted event-by-event, giving estimates of jet transverse energy above the ambient background. The transverse energies of dijets in opposite hemispheres is observed to become systematically more unbalanced with increasing event centrality leading to a large number of events which contain highly asymmetric dijets. This is the first observation of an enhancement of events with such large dijet asymmetries, not observed in proton-proton collisions, which may point to an interpretation in terms of strong jet energy loss in a hot, dense medium.

2

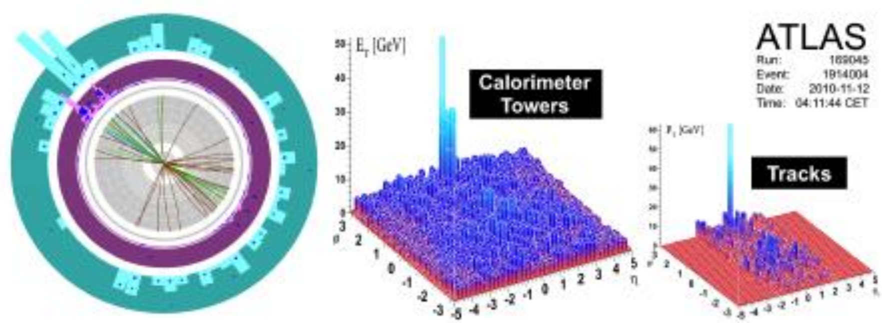

FIG. 1: Event display of a highly asymmetric dijet event, with one jet with $E_T > 100$ GeV and no evident recoiling jet, and with high energy calorimeter cell deposits distributed over a wide azimuthal region. By selecting tracks with $p_T > 2.6$ GeV and applying cell thresholds in the calorimeters ($E_T > 700$ MeV in the electromagnetic calorimeter, and $E > 1$ GeV in the hadronic calorimeter) the recoil can be seen dispersed widely over azimuth.

After event selection, the requirement of a leading jet with $E_T > 100$ GeV and $|\eta| < 2.8$ yields a sample of 1693 events. These are called the "jet selected events". The lead-lead data are also compared with a sample of 17 nb^{-1} of proton-proton collision data [13], which yields 6732 events.

$$A_J = \frac{E_{T1} - E_{T2}}{E_{T1} + E_{T2}}, \Delta\phi > \frac{\pi}{2}$$

where the first jet is required to have a transverse energy $E_{T1} > 100$ GeV, and the second jet is the highest transverse energy jet in the opposite hemisphere with $E_{T2} > 25$ GeV. The average contribution of the under-

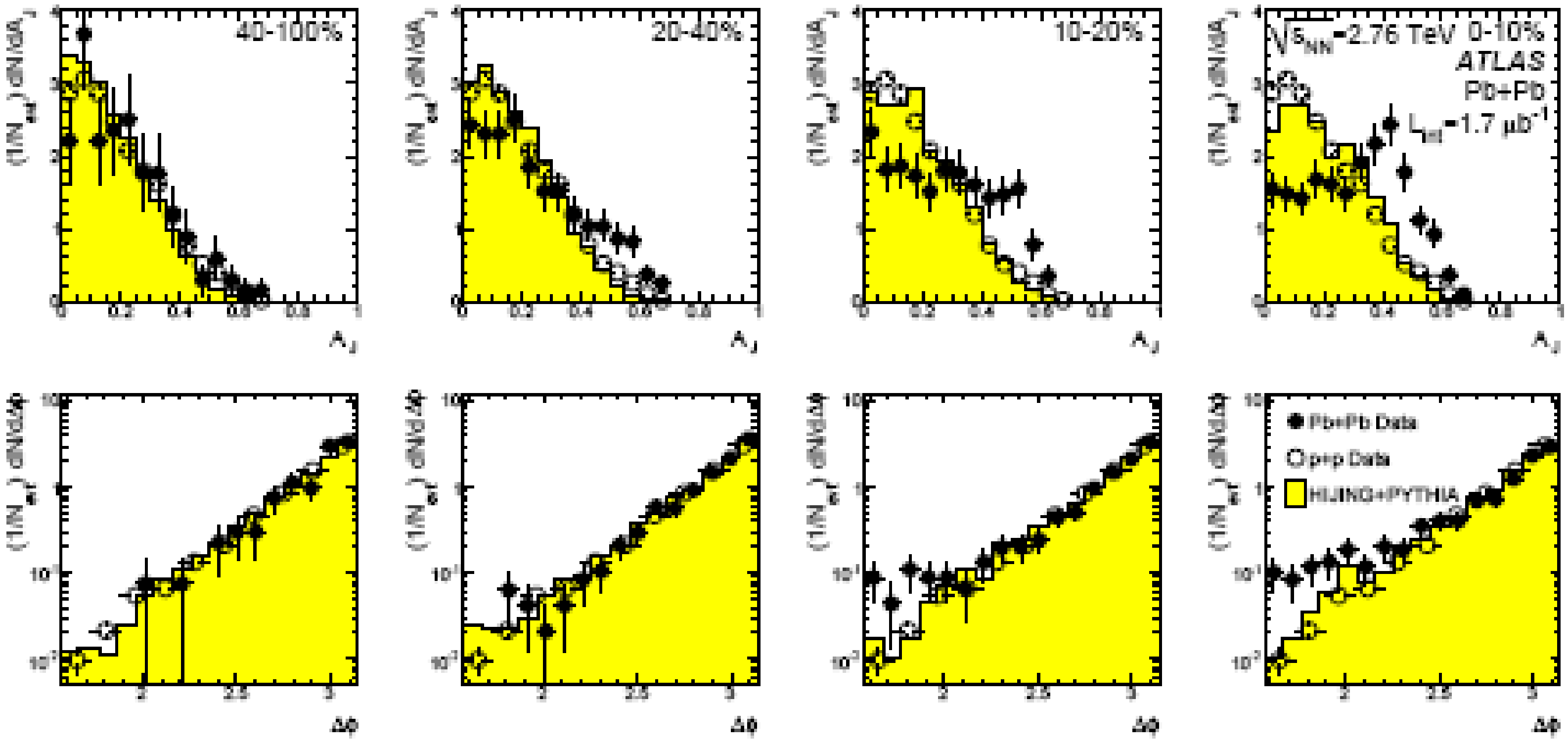

FIG. 3: (top) Dijet asymmetry distributions for data (points) and unquenched HIJING with superimposed PYTHIA dijets (solid yellow histograms), as a function of collision centrality (left to right from peripheral to central events). Proton-proton data from $\sqrt{s} = 7$ TeV, analyzed with the same jet selection, is shown as open circles. (bottom) Distribution of $\Delta\phi$, the azimuthal angle between the two jets, for data and HIJING+PYTHIA, also as a function of centrality.

Jet quenching observed by CMS in heavy-ion collisions – 271110

http://press.web.cern.ch/press/pressreleases/releases2010/pr23.10e.html

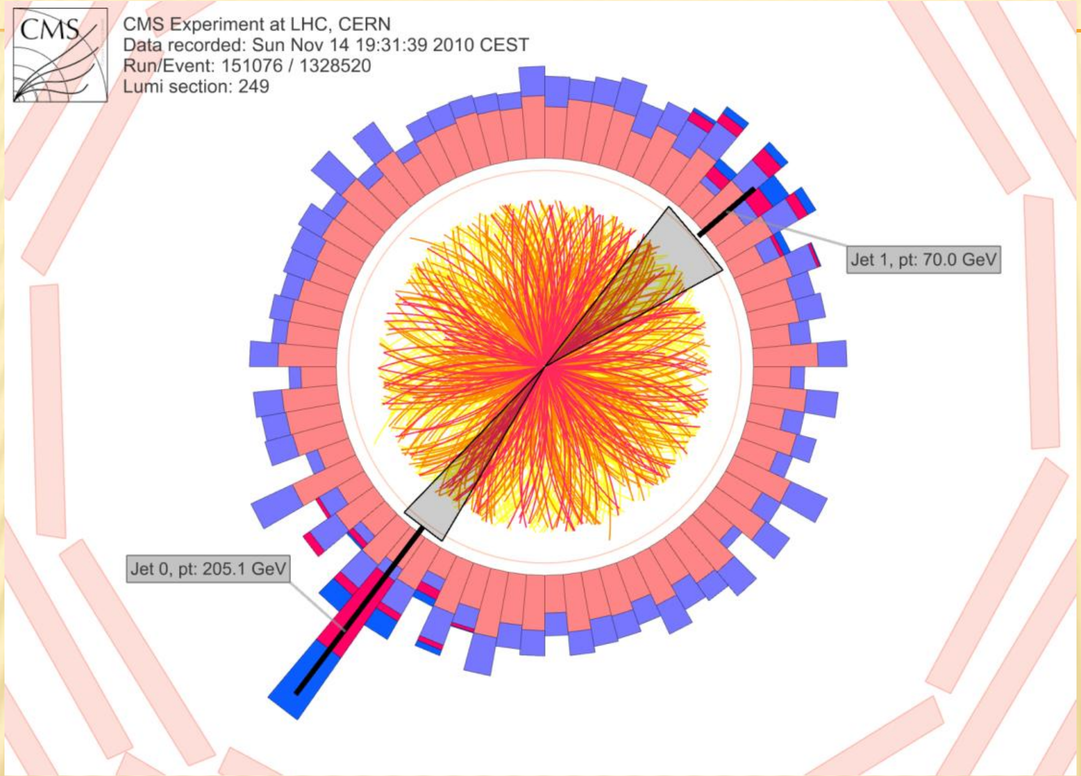

Pt=70 GeV

Pt=205 GeV

Figure 1 LHC lead-lead collision in the CMS detector showing particles (yellow and red tracks) radiating from the collision point. The particles deposit their energy in the calorimeters (salmon, mauve, red and blue towers, with a height proportional to energy). Two back-to-back jets are seen with a large energy asymmetry, as expected from the jet-quenching mechanism.

HI COLLISION - NUCLEAR MODIFICATION FACTOR R_{AA}

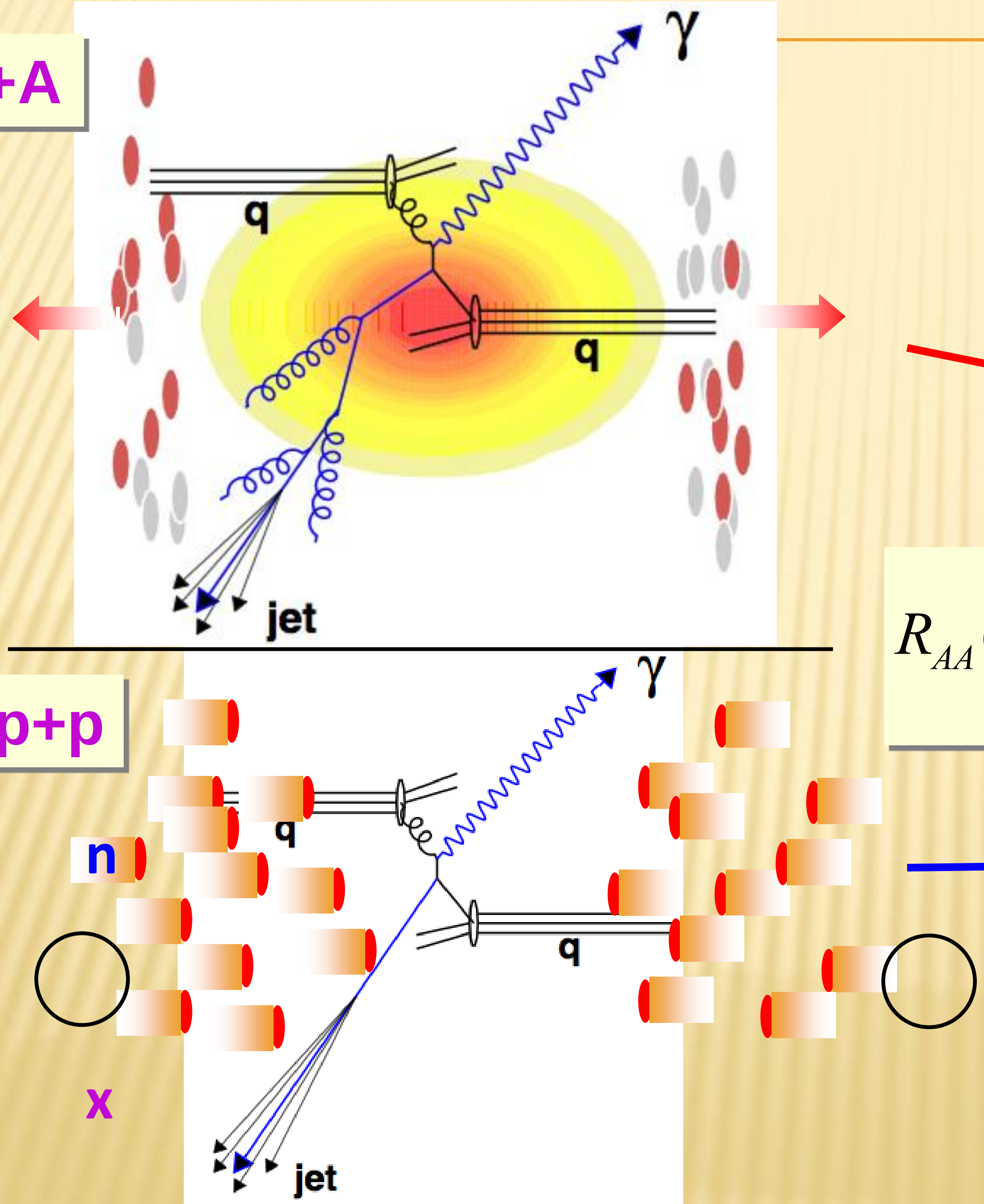

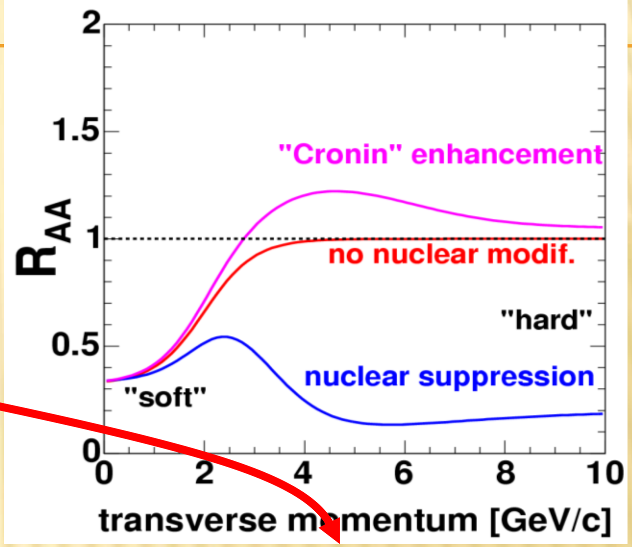

$$R_{AA}(p_T) = \frac{d^2N^{AA} / dp_T d\eta}{\langle N_{binary} \rangle d^2N^{pp} / dp_T d\eta}$$

varies with impact parameter *b*

R. KOLEVATOV:

RFT – a theory of quasiparticle exchanges.

- Ladder (pole) exchange = building block of the apmlitude.
    - Ladder = Reggeon/Pomeron – quasiparticle in $(\vec{b}/\vec{q}_\perp) \times (y = \ln s/s_0)$ space
- A single Pomeron ($\alpha(0) = 1 + \Delta$) exchange breaks unitarity
    - Unitarity is cured by multiP exchanges and R/P interactions

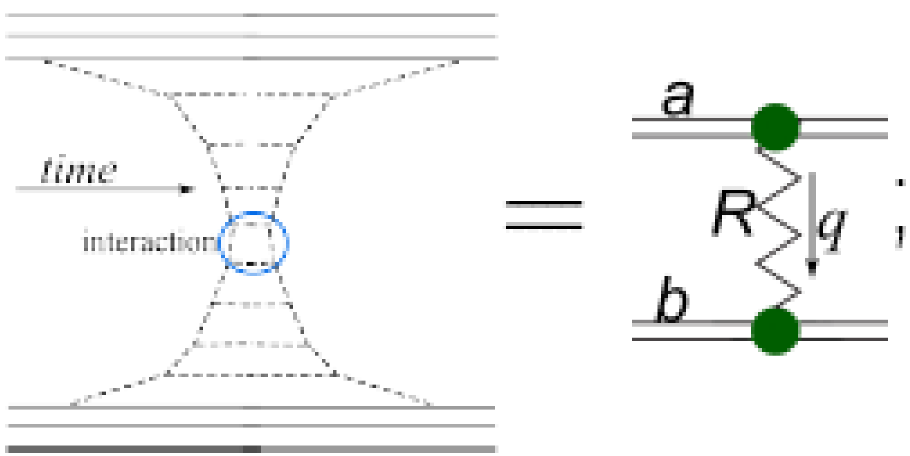

$$A = g_a^R(q^2) D_R(s, q^2) g_b^R(q^2);$$

$$D_R = \eta_R(q^2) \left(\frac{s}{s_0}\right)^{\alpha_R(q^2)}$$

The stochastic model.

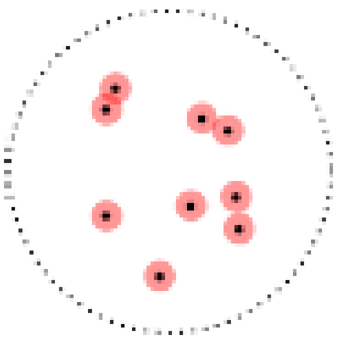

Consider a system of classic "partons" in the transverse plane with:

- Diffusion (chaotical movement) D;
- Splitting (λ – prob. per unit time)
- Death (m_1)
- Fusion ($\sigma_\nu \equiv \int d^2b\, \rho_\nu(b)$)
- Annihilation ($\sigma_{m_2} \equiv \int d^2b\, \rho_{m_2}(b)$)

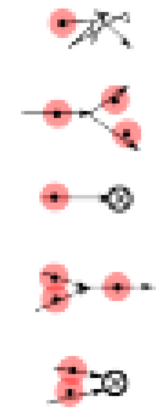

Parton number and positions are described in terms of

probability densities $\rho_N(y, \mathcal{B}_N)$ ($N = 0, 1, \ldots; \mathcal{B}_N \equiv \{b_1, \ldots, b_N\}$)

with normalization $\rho_N(y) \equiv \frac{1}{N!} \int \rho_N(y, \mathcal{B}_N) \prod d\mathcal{B}_N; \quad \sum_0^\infty \rho_N = 1.$

Correspondence RFT–Stochastic model

We use the simplest form of $g(b)$, $p_{m_2}(b)$ and $p_\nu(b)$:

$$p_{m_2}(\mathbf{b}) = m_2\,\theta(a - |\mathbf{b}|); \quad p_\nu(\mathbf{b}) = \nu\,\theta(a - |\mathbf{b}|);$$
$$g(\mathbf{b}) = \theta(a - |\mathbf{b}|);.$$

with a – some small scale; $\epsilon \equiv \pi a^2$.

RFT	stochastic model
Rapidity y	Evolution time y
Slope α'	Diffusion coefficient D
$\Delta = \alpha(0) - 1$	$\lambda - m_1$
Splitting vertex r_{3P}	$\lambda\sqrt{\epsilon}$
Fusion vertex r_{3P}	$(m_2 + \frac{1}{2}\nu)\sqrt{\epsilon}$
Quartic coupling χ	$\frac{1}{2}(m_2 + \nu)\epsilon$

Boost invariance $(\lambda = m_2 + \frac{\nu}{2}) \Leftrightarrow$ equality of fusion and splitting vertices

The effect of loops

Calculations with $\Delta = 0.12$:

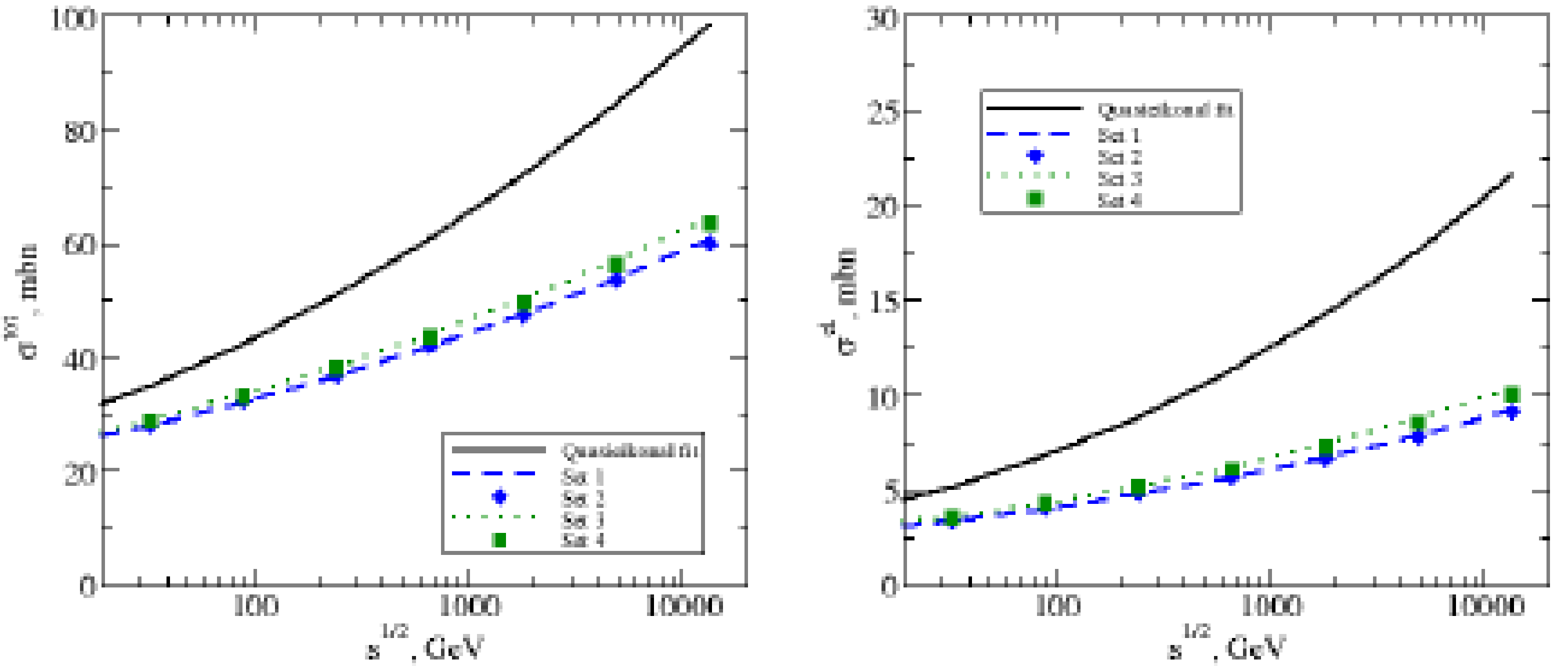

- The growth with $\sqrt{s}$ is suppressed compared to the eikonal.
- The role of $2 \to 2$ coupling is minor.

The effect of loops

Full calculation with $\Delta = 0.165$ and the same couplings vs the quasieikonal fit.

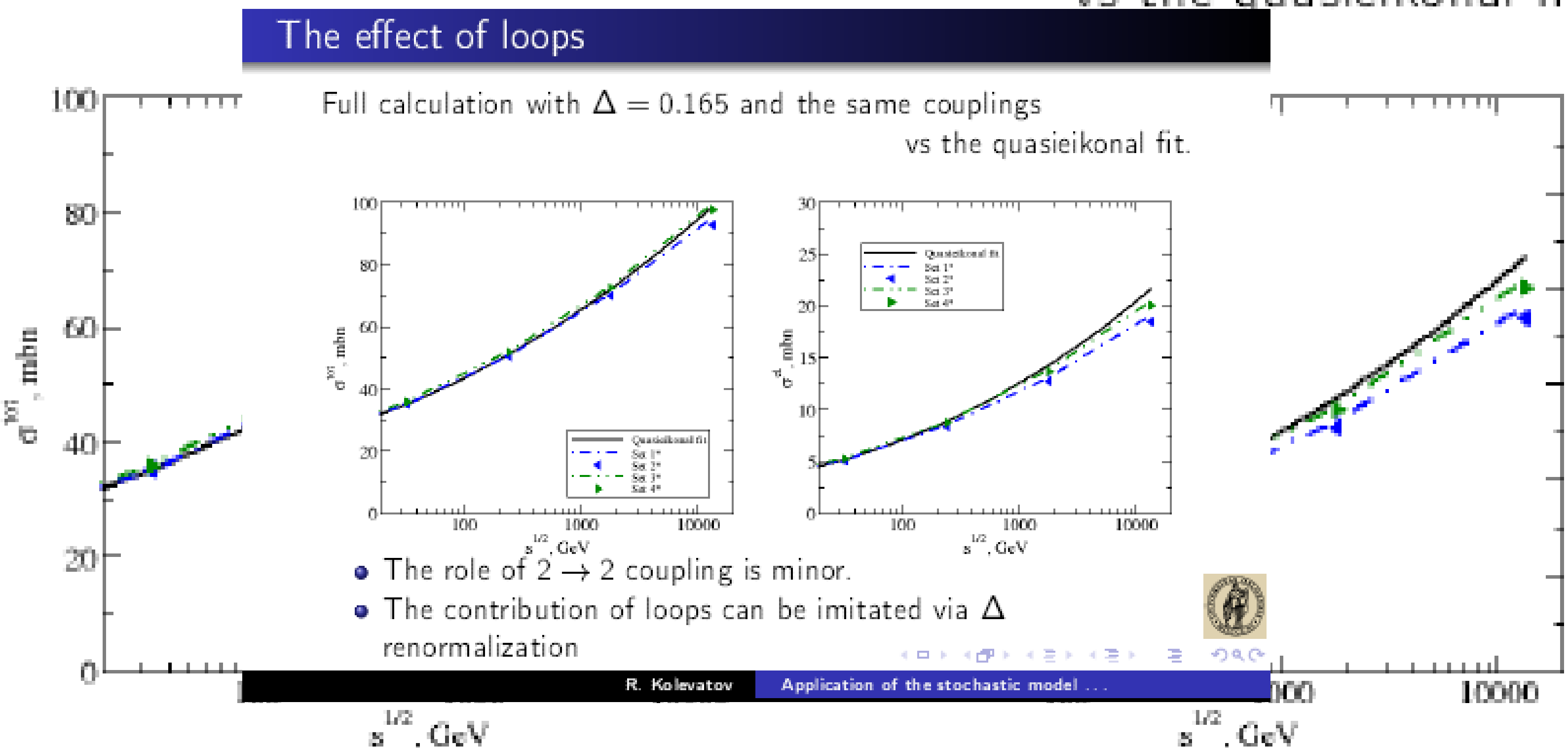

- The role of $2 \to 2$ coupling is minor.
- The contribution of loops can be imitated via Δ renormalization

MC realization: Correlations in double parton distributions at small x. Ch. Flensburg, G. Gustafson, L. Lonnblad, A. Ster JHEP 1106 (2011) 066 .1103.4320 [hep-ph]